

AD-A086 342

HONEYWELL CORPORATE TECHNOLOGY CENTER BLOOMINGTON MN F/G 20/2  
FEASIBILITY OF OPEN TUBE SLIDER GROWTH OF HBCDT FROM TE-RICH 5--ETC(U)  
FEB 80 J L SCHMIT, J E BOWERS F33615-77-C-5142

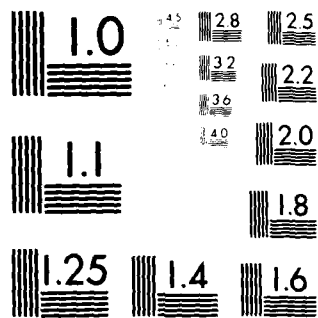
UNCLASSIFIED

AFWAL-TR-80-4068

NL

1 OF 1  
ALL  
COPYRIGHT

END  
DATE  
FILMED  
8-80  
DTIC



MICROCOPY RESOLUTION TEST CHART  
NATIONAL BUREAU OF STANDARDS-1963-A

ADA U86342

✓  
**LEVEL**

AFWAL-TR-80-4068

**FEASIBILITY OF OPEN TUBE SLIDER GROWTH OF HgCdTe  
FROM Te-RICH SOLUTION**

Joseph L. Schmit and John E. Bowers  
Honeywell Inc.  
Corporate Technology Center  
Bloomington, Minnesota 55420

February 1980

Technical Report AFWAL-TR-80-4068 for period  
January 1979 — January 1980

Approved for public release; distribution unlimited.

AIR FORCE MATERIALS LABORATORY  
AIR FORCE WRIGHT AERONAUTICAL LABORATORIES  
AIR FORCE SYSTEMS COMMAND  
WRIGHT-PATTERSON AIR FORCE BASE, OHIO 45433



DDC FILE COPY

80 7 2 008

## **Notice**

When Government drawings, specifications, or other data are used for any purpose other than in connection with a definitely related Government procurement operation, the United States Government thereby incurs no responsibility nor any obligation whatsoever; and the fact that the government may have formulated, furnished, or in any way supplied the said drawings, specifications, or other data, is not to be regarded by implication or otherwise as in any manner licensing the holder to any other person or corporation, or conveying any rights or permission to manufacture, use, or sell any patented invention that may in any way be related thereto.

This report has been reviewed by the Information Office (IO) and is releasable to the National Technical Information Service (NTIS). At NTIS, it will be available to the general public, including foreign nations.

This technical report has been reviewed and is approved for publication.

ROBERT L. HICKMOTT, Project Engineer  
Laser and Optical Materials Branch  
Electromagnetic Materials Division  
Air Force Materials Laboratory

**FOR THE COMMANDER**

DR. G. EDWARD KUHL, Chief  
Laser and Optical Materials Branch  
Electromagnetic Materials Division  
Air Force Materials Laboratory

"If your address has changed, if you wish to be removed from our mailing list, or if the addressee is no longer employed by your organization please notify AFWAL/LOP, WPAFB, OH 45433 to help us maintain a current mailing list."

Copies of this report should not be returned unless return is required by security considerations, contractual obligations, or notice on a specific document.

UNCLASSIFIED

SECURITY CLASSIFICATION OF THIS PAGE (WHEN DATA ENTERED)

REPORT DOCUMENTATION PAGE		READ INSTRUCTIONS BEFORE COMPLETING FORM
1. REPORT NUMBER AFWAL-TR-80-4068	2. GOV'T ACCESSION NUMBER AD-A086342	3. RECIPIENT'S CATALOG NUMBER (9)
4. TITLE (AND SUBTITLE) Feasibility of Open Tube Slider Growth of HgCdTe from Te-Rich Solution.		5. DATE OF REPORT/PERIOD COVERED Interim Technical Report, January 79 - December 79 Jan 80
7. AUTHOR(S) Joseph L. Schmitz and John E. Bowers		8. CONTRACT OR GRANT NUMBER(S) F33615-77-C-5142
9. PERFORMING ORGANIZATIONS NAME/ADDRESS Honeywell Inc., Corporate Technology Center 10701 Lyndale Ave. So. Bloomington, MN 55420		10. PROGRAM ELEMENT, PROJECT, TASK AREA & WORK UNIT NUMBERS Program Element; 62102F Project/Task/Work Unit: 2423/01/08
11. CONTROLLING OFFICE NAME/ADDRESS AIR FORCE MATERIALS LABORATORY (LPO) Air Force Systems Command Wright-Patterson Air Force Base, Ohio 45433		12. REPORT DATE February 1980
14. MONITORING AGENCY NAME/ADDRESS (IF DIFFERENT FROM CONT. OFF.)  12 65		13. NUMBER OF PAGES 11
		15. SECURITY CLASSIFICATION (OF THIS REPORT) UNCLASSIFIED
		15a. DECLASSIFICATION DOWNGRADING SCHEDULE
16. DISTRIBUTION STATEMENT (OF THIS REPORT) Approved for public release; distribution unlimited.		
17. DISTRIBUTION STATEMENT (OF THE ABSTRACT ENTERED IN BLOCK 20, IF DIFFERENT FROM REPORT) 16 2423 17 01		
18. SUPPLEMENTARY NOTES		
19. KEY WORDS (CONTINUE ON REVERSE SIDE IF NECESSARY AND IDENTIFY BY BLOCK NUMBER) Mercury-Cadmium Telluride Liquid Phase Epitaxy Te-Rich Open Tube-Slider		
20. ABSTRACT (CONTINUE ON REVERSE SIDE IF NECESSARY AND IDENTIFY BY BLOCK NUMBER) This report covers the feasibility demonstration of the growth of Hg <sub>1-x</sub> Cd <sub>x</sub> Te by liquid phase epitaxy from Te-rich solution at atmospheric pressure. Growth parameters are calculated from the phase diagram, measurement methods are described for determining layer thickness, uniformity, composition, and electrical properties. Substrate preparation and the growth process are described. Comparisons are made with growth from Hg-rich and HgTe-rich solutions. Layers as thin as 2 $\mu$ m.		

HD-168 REV 11/74

DD FORM 1 JAN 73 1473 EDITION OF 1 NOV 55 IS OBSOLETE

UNCLASSIFIED  
SECURITY CLASSIFICATION OF THIS PAGE (WHEN DATA ENTERED)

407493

Hhner

*square*  
*microns*  
**UNCLASSIFIED**

**SECURITY CLASSIFICATION OF THIS PAGE (WHEN DATA ENTERED)**

20 ✓ Abstract (Continued)

and as thick as 54  $\mu\text{m}$  have been grown; most layers are 1  $\text{cm}^2$  but some are 2x3  $\text{cm}^2$ . We conclude that LPE growth is feasible from Te-rich solution at atmospheric pressure and are continuing our efforts to optimize the growth parameters and to increase the layer area. *square*

**UNCLASSIFIED**

**SECURITY CLASSIFICATION OF THIS PAGE (WHEN DATA ENTERED)**

## Foreword

The first 17 months of contract F33615-77-C-5142 were covered in AFML-TR-79-4036 dated February 1979 and titled "Minority Carrier Lifetime and Diffusion Length in p-type Mercury Cadmium Telluride." The next 12 months of this contract covering all of 1979 are reported in this report. Robert L. Hickmott of AFML is the contract monitor. The emphasis has changed from measuring minority carrier properties to demonstrating the feasibility of liquid phase epitaxial (LPE) growth of  $\text{Hg}_{1-x}\text{Cd}_x\text{Te}$  from Te-rich solution using an open tube slider type system.

The authors of this report wish to thank the Technical staff at the Honeywell Corporate Technology Center (HCTC) for their competent support. These include technicians Larry Miller who machined most of the LPE system parts, Jake DeKruff who fashioned the quartz parts, Dick George and Char Pickering who did the SEM evaluations, Curt Knudson who did the x-ray orientation work, and Nancy Newkument who grew the layers. Students who helped with the work on a parttime basis were Suk Ki Kim, Jerry Lindberg, John Wilson and Faith Eldal. Dr. Walter Scott has been a steady and valued consultant.

The diode fabrication and evaluation was done at the Honeywell Electro Optics Center under the direction of Dr. Paul LoVecchio.

Handwritten: 79-11-14

Accession For	
NTIS	<input checked="checked" type="checkbox"/>
DDI TAB	<input type="checkbox"/>
Unannounced	<input type="checkbox"/>
Justification	
By	
Distribution/	
Availability Codes	
Dist	Initial and/or special
A	

## Table of Contents

Section		Page
1	INTRODUCTION	1
2	THEORY	2
	2.1 Hg Containment	2
	2.2 Theory of Growth	4
3	MEASUREMENT METHODS	15
	3.1 Growth Solution Uniformity	15
	3.2 Layer Thickness	15
	3.3 Layer Composition	16
	3.4 Electrical Properties	20
4	LPE METHOD	21
	4.1 Substrate Preparation	21
	4.2 Slider System	21
	4.3 Growth Procedure	21
5	RESULTS AND CONCLUSIONS	23
	REFERENCES	29
APPENDIX A	LPE GROWTH OF $\text{Hg}_{0.60}\text{Cd}_{0.40}\text{Te}$ FROM Te-RICH SOLUTION	33
APPENDIX B	CHARACTERIZATION OF LPE GROWN $\text{Hg}_{1-x}\text{Cd}_x\text{Te}$	36
APPENDIX C	COMPARISON OF $\text{Hg}_{0.6}\text{Cd}_{0.4}\text{Te}$ LPE LAYER GROWTH FROM Te-, Hg- AND $\text{HgTe}$ -RICH SOLUTIONS	51



## List of Illustrations

Figure		Page
1	T-x Phase Diagram for $\text{Hg}_{1-x}\text{Cd}_x\text{Te}$	8
2	Segregation Coefficient of $\text{Hg}_{1-x}\text{Cd}_x\text{Te}$	9
3	Calculated Change in Cd Concentration of a Solution Precipitating $\text{Hg}_{1-x}\text{Cd}_x\text{Te}$ Due to Supercooling $\Delta T^\circ\text{C}$	10
4	Density of Growth Solutions and Solid $\text{Hg}_{1-x}\text{Cd}_x\text{Te}$ as a Function of Composition Grown	12
5	Layer Thickness Grown per Degree Supercooling as a Function of Composition	13
6	Change in Composition as a Function of the Layer Thickness Grown from a Solution 3mm Thick	14
7	Two Photomicrographs of the Surface of Layer HCT74	17
8	A Polished Cross-Section of Layer HCT75 Showing the Color Difference Between Layer and Substrate, and the Smooth Interface Boundary	18
9	A Talysurf Trace of Layer HCT74 Showing the Signatures of Various Defects	18
10	IR Transmission Through Layer HCT51 as a Function of Photon Energy	19
11	Variation of CdTe Mole Fraction With Depth into an LPE Layer	24
12	SEM Profile of an LPE Layer	25
13	$R_0A_j$ for 2 Diodes Made from $\text{Hg}_{0.695}\text{Cd}_{0.30}\text{Te}$ Layer HCT41	26

## List of Tables

Table		Page
1	Calculated Loss of Hg by Diffusion	4
2	Liquidus Slopes from Thermal Arrest Data	9
3	Density of Growth Solution and Solid $\text{Hg}_{1-x}\text{Cd}_x\text{Te}$	11
4	Tie Line Parameters	27

## Section 1 Introduction

This contract is an extension of the work we did in 1978 to determine the minority carrier lifetime and diffusion length in bulk grown  $\text{Hg}_{0.6}\text{Cd}_{0.4}\text{Te}$ . One of the recommendations of that work was that a crystal growth method alternative to quench-anneal be developed. LPE growth was recommended in the hope that the lower growth temperature inherent in LPE growth would lead to the formation of fewer defects and recombination centers. This report documents that, although we have not yet achieved that goal, we have demonstrated the feasibility of growing  $\text{Hg}_{1-x}\text{Cd}_x\text{Te}$  at atmospheric pressure from a Te-rich solution.

Section 2 calculates the amount of Hg we can expect to lose via diffusion and shows how the segregation coefficient, solution composition, density, and composition grown depend on super cooling and the thickness of layer grown. Section 3 details the methods used to determine the properties of interest. Section 4 outlines the growth process, including the substrate preparation technique. Section 5 and the three appendices give the results achieved during this past year. (The appendices are three papers we wrote during 1979 covering the LPE growth of  $\text{HgCdTe}$ .) The general conclusion of this work is that we have demonstrated the feasibility of growing  $\text{Hg}_{1-x}\text{Cd}_x\text{Te}$  by LPE in a slider-type system at atmospheric pressure. The layers grown are shown to be uniform in composition across a layer and with depth into a layer.

## Section 2 Theory

### 2.1 Hg CONTAINMENT

We are growing  $\text{Hg}_{1-x}\text{Cd}_x\text{Te}$  by LPE at atmospheric pressure. The high Hg vapor pressure over HgTe or over an Hg-rich solution dictates that growth be from a Te-rich solution. At 500°C the Hg vapor pressure over Te saturated  $\text{Hg}_{0.6}\text{Cd}_{0.4}\text{Te}$  is 0.1atm.<sup>1</sup> We assume that the Hg pressure over a Te-rich solution in equilibrium with  $\text{Hg}_{0.6}\text{Cd}_{0.4}\text{Te}$  will be the same. Even at this relatively low Hg pressure some Hg will be lost and steps must be taken to control the loss. This section calculates the Hg that will be lost by diffusion through the space between the stator and slider of our LPE growth apparatus.

Frick's first law of diffusion<sup>2</sup> is

$$J = -D \frac{\partial C}{\partial x} A \quad (1)$$

where

$A$  = the cross-sectional area perpendicular to flow,  $\text{cm}^2$

$\frac{\partial C}{\partial x}$  = the concentration gradient,  $\text{gm}/\text{cm}^4$

$D$  = the diffusion coefficient,  $\text{cm}^2/\text{s}$

$J$  = the diffusion flow,  $\text{gm}/\text{s}$ .

At 0°C and one atmosphere pressure,  $D_0 = 0.53\text{cm}^2/\text{s}$  (Jost, p. 413) for Hg vapor in  $\text{H}_2$  gas. For gases,

$$D = D_0 \left( \frac{T}{T_0} \right)^{(3/2+s)} \quad (2)$$

where

$s = 1/2$  for Maxwellian molecules

$s = 0$  for rigid spheres.

- 
1. J.P. Schwartz, Ph.D. Thesis, Marquette University, p. 99, (1977).
  2. W. Jost, *Diffusion in Solids, Liquids and Gases*, Academic Press, NY (1952).

We use real gases,  $0 \leq s \leq 1$ , with  $s$  usually near  $1/2$ . We use  $s = 1/2$  so that at  $500^\circ\text{C}$

$$D = D_0 (T/T_0)^2 = 0.53 (773/273)^2 = 4.25 \text{ cm}^2/\text{s}. \quad (3)$$

(Note: In solids  $D$  has an exponential dependence on  $T$ , that is,  $D = D_0 e^{-Q/T}$ ).

The ideal gas law is  $pV = nRT$ , where  $R = 82 \text{ atm cm}^3/^\circ\text{K mole}$ . Thus at  $0.1 \text{ atm Hg}$  pressure the Hg concentration is

$$C = \frac{n (\text{moles})}{V (\text{cm}^3)} M (\text{gm/mole}) = \frac{PM}{RT} = 3.2 \times 10^{-4} (\text{gm/cm}^3) \quad (4)$$

Outside the slider, the Hg concentration is zero. For our slider No. 1, diffusion occurs over a length of  $0.5 \text{ cm}$  through an area of  $0.003 \text{ cm} \times 15 \text{ cm}$ . Therefore the loss of Hg at  $500^\circ\text{C}$  should be:

$$J = -DA \frac{\partial C}{\partial x} = \frac{4.25 (3.2 \times 10^{-4} - 0) 0.003 \times 15}{0.5} = 1.22 \times 10^{-4} \frac{\text{g}}{\text{s}} = \frac{440 \text{ mg}}{\text{hr}} \quad (5)$$

A typical growth run takes about an hour and the growth solution weighs about  $1.5 \text{ gm}$ ; thus, a  $400 \text{ mg}$  loss is intolerable. Slider No. 2 incorporates an extra chamber containing HgTe between the growth solution and the  $\text{H}_2$  stream outside the slider. This extra chamber provides a source of Hg that pressurizes the growth solution, reducing the diffusion loss by an order of magnitude.

Table 1 lists the calculated Hg loss from the three sliders built to date. The exact clearance between the cover and the slider and between the slider and the stator cannot be measured easily. The clearance is obviously zero in some places but the fit is not perfect. We have used an average clearance of  $0.003 \text{ cm}$  in these calculations. The dynamics of dissociation of HgTe into Hg and Te to provide the Hg pressure are not known. If the HgTe does not dissociate fast enough to keep the outer chamber pressurized with Hg, then some Hg will diffuse from the growth solution well. For this calculation we have arbitrarily assumed that the pressure over the Hg source is  $0.9$  times the pressure in the growth well. The point of this calculation is to show that the newer sliders have the potential of greatly reducing the Hg loss.

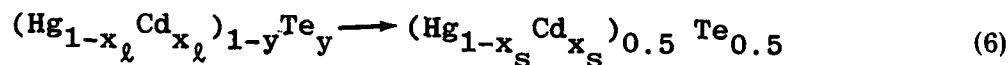
Table 1. Calculated Loss of Hg by Diffusion

Slider (No.)	Loss from Hg Source (mg/hr)	Loss from Growth Well Under Plug (mg/hr)	Loss from Growth Well if $P_{\text{Hg}} = 0.9P_{\text{well}}$ (mg/hr)	Loss from Growth Well if $P_{\text{Hg}} = P_{\text{well}}$ (mg/hr)
1	440	150	75	65
2	880	270	27	0
3	750	130	13	0

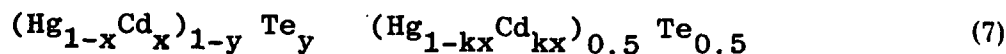
## 2.2 THEORY OF GROWTH

This calculation was originally made by Jack Mroczkowski<sup>3</sup> of the Honeywell Electro-Optical Center and is repeated here because of its general applicability. We have changed the form somewhat to suit our needs better.

Liquid Te-rich solution precipitates  $\text{Hg}_{1-x}\text{Cd}_x\text{Te}$  according to the relationship



where  $x_l$  is the ratio of Cd to Cd + Hg in the liquid and  $x_s$  is the same ratio for the solid grown. The segregation coefficient,  $k$ , is defined as  $x_s/x_l$ . The rest of this discussion uses  $x$  for  $x_l$ , and  $x_s$  to refer to the solid. In the formula for stoichiometric  $\text{Hg}_{1-x}\text{Cd}_x\text{Te}$ ,  $x$  still refers to  $x_{\text{solid}}$ . Relationship 1 becomes



If we use the method of finite differences, we can calculate changes in  $x$  and  $y$  as functions of growth parameters such as liquidus slopes, segregation coefficient, and temperature difference. Consider  $M$  moles of saturated  $(\text{Hg}_{1-x}\text{Cd}_x)_{1-y}\text{Te}_y$  that precipitates  $\Delta M$  moles of  $(\text{Hg}_{1-kx})_{0.5}\text{Te}_{0.5}$  when cooled  $\Delta T$ . If we define  $\Delta M$  as the small amount of the liquid that precipitates, then Relationship 7 can be rewritten as

3. J.A. Mroczkowski, Contract F33615-78-C-5156, Letter Report No. 11 (July-August, 1979).

$$\begin{array}{c} \text{Hg}_{M(1-x)(1-y)} \text{Cd}_{Mx(1-y)} \text{Te}_{My} \rightarrow \text{Hg} \frac{\Delta M (1-kx)}{2} \\ \text{Cd} \frac{\Delta M kx}{2} \text{Te} \frac{\Delta M}{2} \end{array} \quad (8)$$

To get an equality we consider that only the *change* in the liquid becomes the solid and that Hg, Cd, and Te can be treated independently. Thus the change in the Hg content of the liquid solution is

$$\Delta \{M(10x)(106)\} = \frac{\Delta M (1-kx)}{2} \quad (9)$$

The change in the Cd content of the liquid is

$$\Delta \{Mx(1-y)\} = \frac{\Delta M(kx)}{2} \quad (10)$$

Similarly, for Te

$$\Delta \{My\} = \frac{\Delta M}{2} \quad (11)$$

These three equations are not independent; therefore, we will carry through the differentiation of the left side of only the last two equations and divide through by M:

$$\left(\frac{\Delta M}{M}\right) x (1-y) + \Delta x (1-y) - \Delta y x = \left(\frac{\Delta M}{M}\right) \frac{kx}{2} \quad (10')$$

$$\Delta y + \left(\frac{\Delta M}{M}\right) y = \frac{1}{2} \left(\frac{\Delta M}{M}\right) \quad (11')$$

In addition, the liquidus temperature,  $T_\ell$ , is a function of  $x$  and  $y$ :

$$T_\ell = f(x, y) \quad (12)$$

Dropping the subscript and differentiating, we get

$$\Delta T = \left. \frac{\partial T}{\partial x} \right|_y \Delta x + \left. \frac{\partial T}{\partial y} \right|_x \Delta y \quad (13)$$

where the partial derivatives are simply the slopes of the liquidus surface  $m_x$  and  $m_y$  at constant  $y$  and constant  $x$ , respectively.

Equations 10', 11' and 12 are three independent equations relating  $\Delta x$ ,  $\Delta y$ , and  $(\Delta M/M)$ . They can be rearranged as follows:

$$(1-y) \Delta x - x \Delta y + [x(1-y) - kx/2] (\Delta M/M) = 0 \quad (14)$$

$$0 \Delta x + 1 \Delta y + [y-1/2] (\Delta M/M) = 0 \quad (15)$$

$$m_x \Delta x + m_y \Delta y + 0 (\Delta M/M) = \Delta T \quad (16)$$

Solving for  $\Delta x$ ,  $\Delta y$ , and  $(\Delta M/M)$ , we get

$$\Delta x = \frac{x(k-1) \Delta T}{m_x x(k-1) - m_y (2y-1)(1-y)} \quad (17)$$

$$\Delta y = \frac{-(2y-1)(1-y) \Delta T}{m_x x(k-1) - m_y (2y-1)(1-y)} \quad (18)$$

$$\frac{\Delta M}{M} = \frac{2(1-y) \Delta T}{m_x x(k-1) - m_y (2y-1)(1-y)} \quad (19)$$

These equations are identical to J. Mroczkowski's (see footnote 3, above).

The change in Cd concentration as material precipitates is given by

$$\Delta [C_{Cd}] = \Delta [x(1-y)] = (1-y)\Delta x - x\Delta y \quad (20)$$

Substituting Equations (17) and (18) in Equation (20), we get

$$\Delta C_{Cd} = \frac{(k + 2y - 2)(1-y)x \Delta T}{m_x x(k-1) - m_y (2y-1)(1-y)} \quad (21)$$

The liquidus slope with respect to Cd is thus

$$\frac{\Delta T}{\Delta C_{Cd}} = \frac{m_x x(k-1) - m_y (2y-1)(1-y)}{(1-y)x(k+2y-2)} = \frac{\partial T}{\partial C_{Cd}} = m_{Cd} \quad (22)$$



It now remains to estimate some of the constants so that we can calculate LPE film thickness and composition as a function of thickness. Ted Harman<sup>4</sup> has indicated that the segregation coefficient is the same for growth from Te solution as it is for growth along the pseudo-binary. The best data for the pseudo-binary<sup>5</sup> is plotted in Figure 1 along with less extensive data<sup>6,7,8</sup>. Figure 2 is a plot of the segregation coefficient as a function of composition taken from Figure 1. For solidus compositions between 0.1 and 0.5,  $k=3.5\pm0.1$ . The data represented by triangles will be discussed later.

The slopes  $m_x$  and  $m_y$  are obtained from Mroczkowski's work<sup>9</sup> or from Harman's unpublished work<sup>4</sup>. Table 2 summarizes the slopes taken from their data.

Using these average values of  $k$ ,  $m_x$ , Equation (22) becomes

$$\frac{\Delta C_{Cd}}{\Delta T} = \frac{(1-y) x (1.5 + 2y)}{1583x + 887(2y-1)(1-y)} \quad (23)$$

We evaluated Equation (18) for typical values of  $x$  and  $y$ . The results are shown in Figure 3. Note that  $\Delta C_{Cd}/\Delta T$  is a strong function of both  $x$  and  $y$ . The curve for  $x = 0.9$  begins at  $x_s = 0.25$  in this and future figures because for lower  $x$  values the tie lines connect to Te, not  $Hg_{1-x}Cd_xTe$ .

After a thin layer of  $Hg_{1-x}Cd_xTe$  is grown from a solution, the composition of the solution will change. The question is, what will be the composition that grows in succeeding thin layers? That is, what is

$$\frac{\Delta x_s}{\Delta l/d} = \frac{k \Delta x}{\Delta l/d} \quad (24)$$

where  $\Delta l$  is the layer thickness? The melt depth,  $d$ , is also important because we are assuming complete mixing. Consider growing a layer of  $x = 0.29$  from a solution of  $(Hg_{0.918}Cd_{0.082})_{0.19}Te_{0.81}$ . The density of the layer<sup>7,10</sup> is  $7.43g/cm^3$ . The density of the solution is not known but can be approximated as the average density of the constituents times their weight fraction.

4. Ted Harman of MIT Lincoln Labs, private communication.
5. T.C. Harman and A.J. Strauss, *Physics and Chemistry of II-VI Compounds*, Interscience, p. 784, (1967).
6. J. Steininger, *Journal of Electronic Materials* 5, pp. 299-320, (1976).
7. J. Blair and R. Newnham, *Metallurgy of Elemental and Compound Semiconductors*, Interscience 12, p. 393, (1961).
8. J.L. Schmit and M.W. Scott, unpublished results.
9. J.E. Bowers, J.L. Schmit, and J.A. Mroczkowski, "Characterization of LPE Grown  $Hg_{1-x}Cd_xTe$ ," IRIS Detector Specialty Group Meeting (June 1979), Minneapolis, MN, Figure 3. (Also see Appendix B.)
10. D. Long and J.L. Schmit, *Semiconductors and Semimetals*, Academic Press (1970), 5, Chapter 5, p. 243.

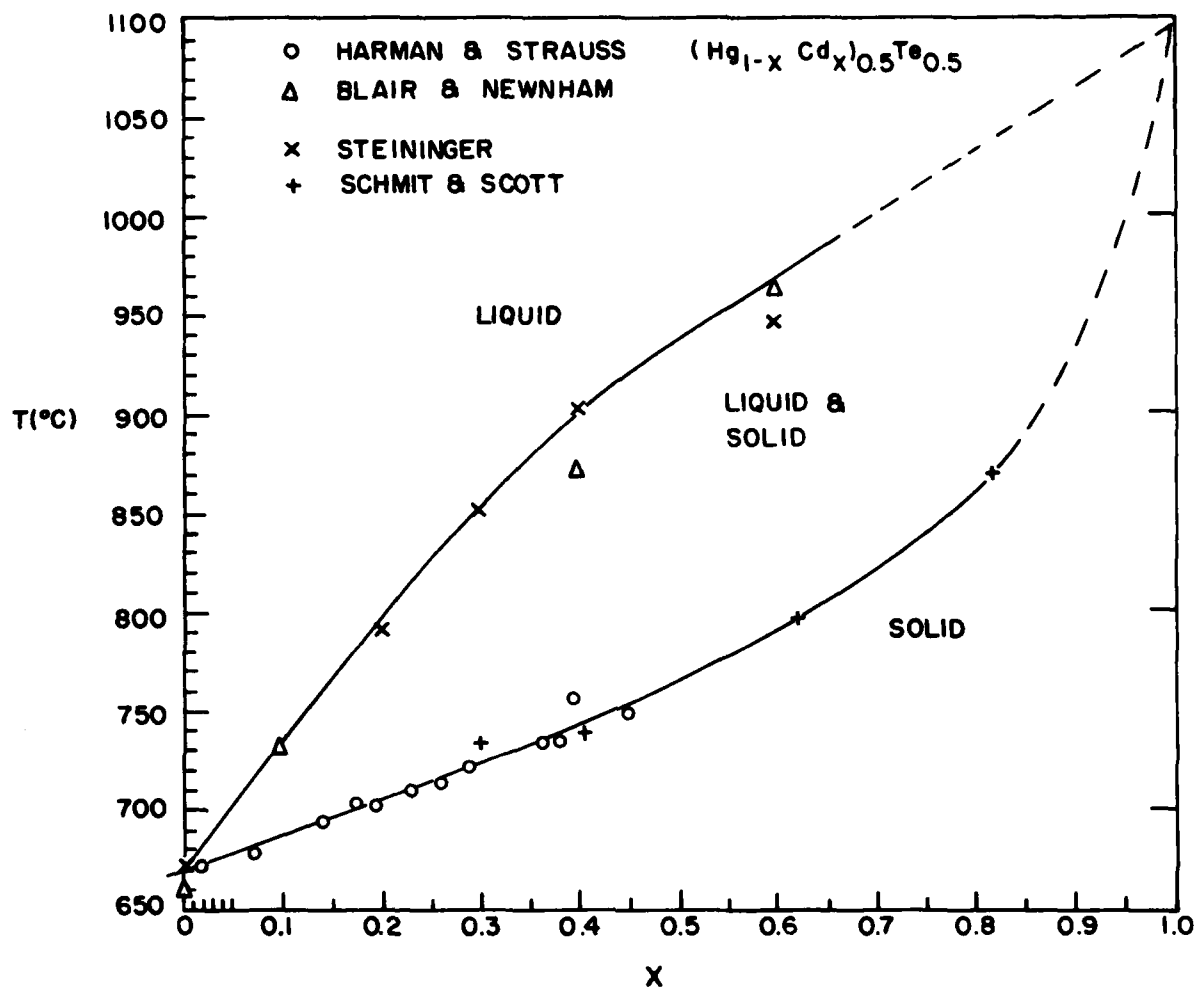


Figure 1. T-x Phase Diagram for  $\text{Hg}_{1-x}\text{Cd}_x\text{Te}$

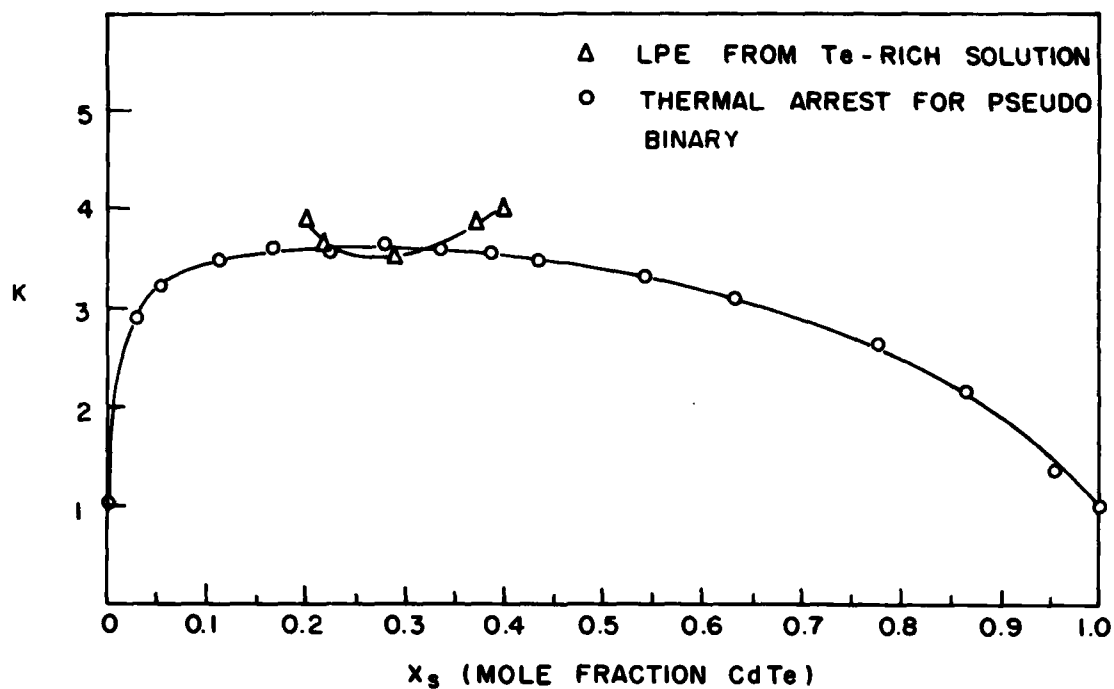


Figure 2. Segregation Coefficient of  $\text{Hg}_{1-x}\text{Cd}_x\text{Te}$ . The circles are from Figure 1; the triangles are from Table 4 in Section 5.

Table 2. Liquidus Slopes from Thermal Arrest Data

Source	$m_x$ ( $^{\circ}\text{C}/\text{mole fraction}$ )	$m_y$ ( $^{\circ}\text{C}/\text{mole fraction}$ )
Mroczkowski	$600 \pm 50$	$-815 \pm 50$
Harman	$667 \pm 50$	$-960 \pm 50$
Average:	633	-887

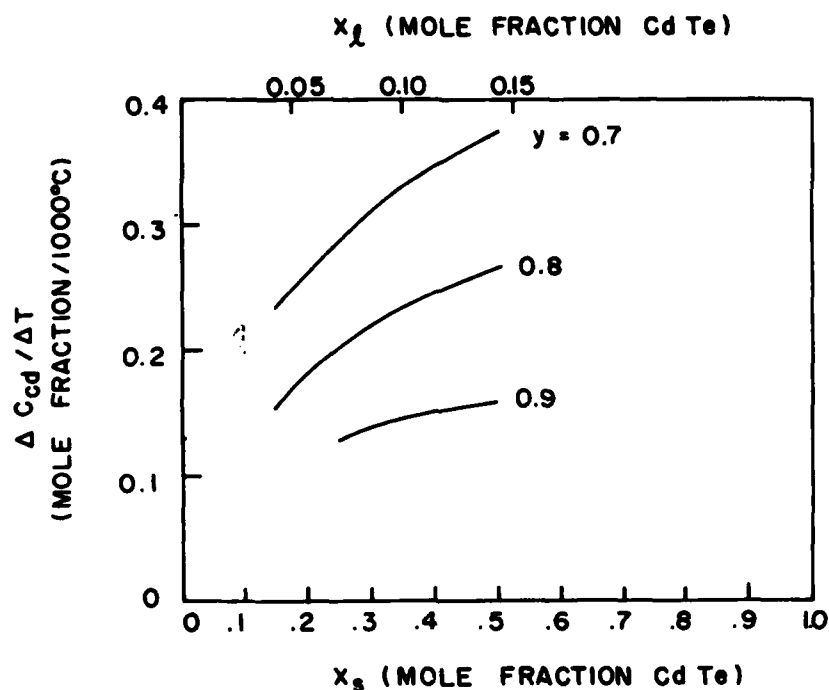


Figure 3. Calculated Change in Cd Concentration of a Solution Precipitating  $\text{Hg}_{1-x_s}\text{Cd}_x\text{Te}$  Due to Supercooling  $\Delta T^\circ\text{C}$

The formula for the solution reduces to  $\text{Hg}_{0.1744}\text{Cd}_{0.0156}\text{Te}_{0.81}$  by mole fraction or  $\text{Hg}_{0.2497}\text{Cd}_{0.0125}\text{Te}_{0.7378}$  by weight fraction. Then

$$\rho_l = 0.2497\rho_{\text{Hg}} + 0.0125\rho_{\text{Cd}} + 0.7378\rho_{\text{Te}} = 8.108 \text{ g/cm}^3 \quad (25)$$

Where  $\rho$  is defined as the density.

If we consider that the Cd and Hg exist as compounds in the liquid, then the formula becomes  $(\text{HgTe})_{0.1744}(\text{CdTe})_{0.0156}\text{Te}_{0.82}$  by mole fractions or  $(\text{HgTe})_{0.4086}(\text{CdTe})_{0.0267}\text{Te}_{0.5647}$  by weight fraction. Therefore

$$\rho_l = 0.4086\rho_{\text{HgTe}} + 0.0267\rho_{\text{CdTe}} + 0.5647\rho_{\text{Te}} = 6.98 \text{ g/cm}^3 \quad (26)$$

using the densities of the solid phases. Chalmers<sup>11</sup> gives the shrinkage of Te, Cd, and Hg upon freezing as 3.2, 4.7, and 3.7 percent, respectively. HgTe and CdTe also shrink upon freezing but we don't have a measure of the amount. Because our growth solutions are mostly Te, we assume a 3.2 percent expansion going from solid to liquid and decrease the liquid densities by that amount. Thus Equation (25) gives  $\rho_\ell = 7.857 \text{ g/cm}^3$ , while Equation (26) gives  $6.764 \text{ g/cm}^3$ . We have determined experimentally that the  $\text{Hg}_{1-x}\text{Cd}_x\text{Te}$  crystals precipitating from solution sink; therefore, the second method of calculating the solution density is better.

Table 3 lists the solid and solution densities calculated for the current range of interest. The solid densities are well known.<sup>7-10</sup> We calculated the solution densities by the method of Equation (26), which assumes CdTe and HgTe molecules are dissolved in Te and that the solution is 3.2 percent less dense than the solid constituents are at the same temperature. The densities are all for room temperature, so we implicitly assume that the coefficient of thermal expansion is the same for  $\text{Hg}_{1-x}\text{Cd}_x\text{Te}$  as for alloys of mainly Te.

Figure 4 is a plot of the densities shown in Table 3. Note that for most choices of  $x$  and  $y$  the solution is less dense than the solid precipitating from it. This means that the liquid layer near a growth interface will be less dense and tend to float, causing convective mixing. Note also that for sufficiently high  $x$  and low  $y$  it should be possible to grow solid material less dense than the solution so that a stable layer can be expected and mixing minimized.

Table 3. Density of Growth Solution and Solid  $\text{Hg}_{1-x}\text{Cd}_x\text{Te}$

$x_s$ (mf CdTe)	$\rho_s$ ( $\text{g/cm}^3$ )	$x$ (mf CdTe)	$\rho_\ell$ for $y=0.7$ ( $\text{g/cm}^3$ )	$\rho_\ell$ for $y=0.8$ ( $\text{g/cm}^3$ )	$\rho_\ell$ for $y=0.9$ ( $\text{g/cm}^3$ )
0.2	7.63	0.057	7.15	6.82	6.45
0.3	7.41	0.086	7.11	6.79	6.44
0.4	7.19	0.114	7.08	6.77	6.42

11. Bruce Chalmers, *Physical Metallurgy*, John Wiley and Sons (1959), p. 79.

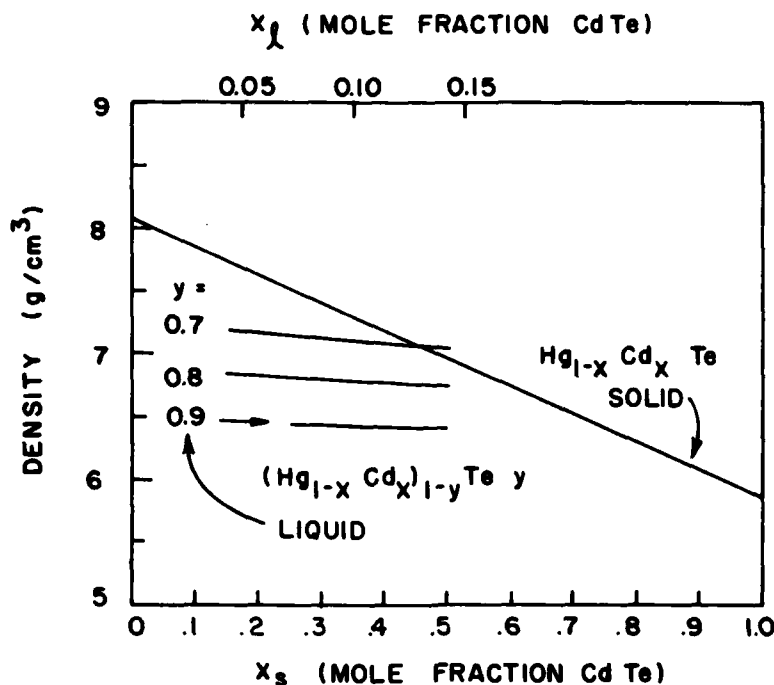


Figure 4. Density of Growth Solutions and Solid  $\text{Hg}_{1-x}\text{Cd}_x\text{Te}$  as a Function of Composition Grown

The main reason for calculating densities, however, was to enable us to predict the change in composition with layer thickness. Table 3 demonstrates that solid and liquid densities are the same within approximately 10 percent; therefore, the layer grown is approximately the same thickness as the solution used up. That is,

$$\frac{\Delta M}{M} = \frac{\Delta \ell}{d} \quad (27)$$

where  $\Delta \ell$  is the thickness of the layer grown and  $d$  is the depth of the solution from which it is grown. Combining Equation (19) with Equation (27) and using the typical depth of 3 mm, we find the thickness of layer grown due to supercooling  $\Delta T^\circ\text{C}$  is

$$\Delta \ell = \left( \frac{\Delta M}{M} \right) d = \frac{2(1-y) \Delta T d}{m_x x(k-1) - m_y(2y-1)(1-y)} = \frac{6000(1-y) \Delta T}{1583x + 887(2y-1)(1-y)} \quad (28)$$

Equation (23) has been plotted in Figure 5, which gives layer thickness expected per °C supercooling as a function of  $x$  and  $y$ , assuming a 3 mm thick melt and complete mixing.

The rate at which the composition of the solid freezing out changes with layer thickness is  $\Delta x_s / \Delta l$ . We have  $\Delta x$  from Equation (17) and can multiply it by  $k$  to get  $\Delta x_s$ , and  $\Delta l$  is given in Equation (28). We then have

$$\frac{\Delta x_s}{\Delta l} = \frac{k x}{\left(\frac{\Delta M}{M}\right) d} = \frac{k x (k-1)}{2d (1-y)} \quad (29)$$

For  $k = 3.5$  and  $d = 3000 \mu\text{m}$ ,

$$\frac{\Delta x_s}{\Delta l} = \frac{35}{24000} = \frac{x}{(1-y)} \quad \frac{\text{mole fraction}}{\mu\text{m}} \quad (30)$$

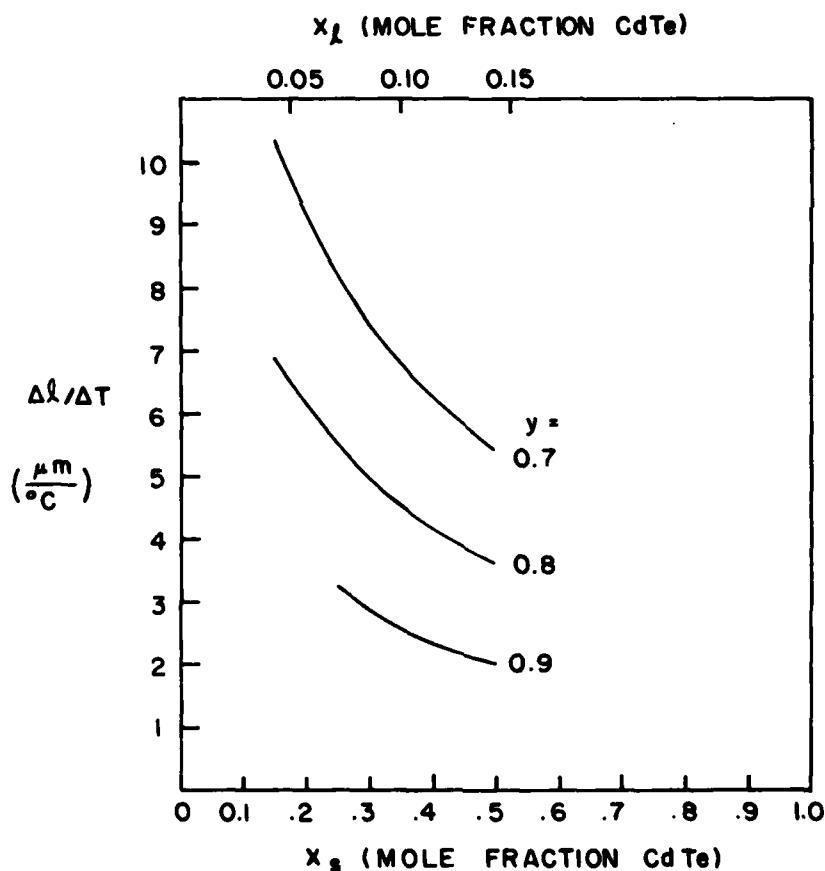


Figure 5. Layer Thickness Grown per Degree Supercooling as a Function of Composition

Equation (30) is plotted in Figure 6 for typical values of  $x$  and  $y$ . For example, Figure 6 predicts that the change in composition for a 20- $\mu\text{m}$  thick layer of  $\text{Hg}_{0.71}\text{Cd}_{0.29}\text{Te}$  grown from a solution with  $y = 0.8$  is

$$\Delta x_s = \frac{\Delta x_s}{\Delta l} \Delta l = (6 \times 10^{-4}) 20 = \quad (31)$$

0.012 mole fraction CdTe

That is, assuming complete mixing of the growth solution, the grown layer would change from 0.290 to 0.278 in 20  $\mu\text{m}$ .

This section has calculated many of the relationships between material parameters involved in liquid phase epitaxy of  $\text{Hg}_{1-x}\text{Cd}_x\text{Te}$ . The results have been plotted to provide convenient comparison with the results of later experiments.

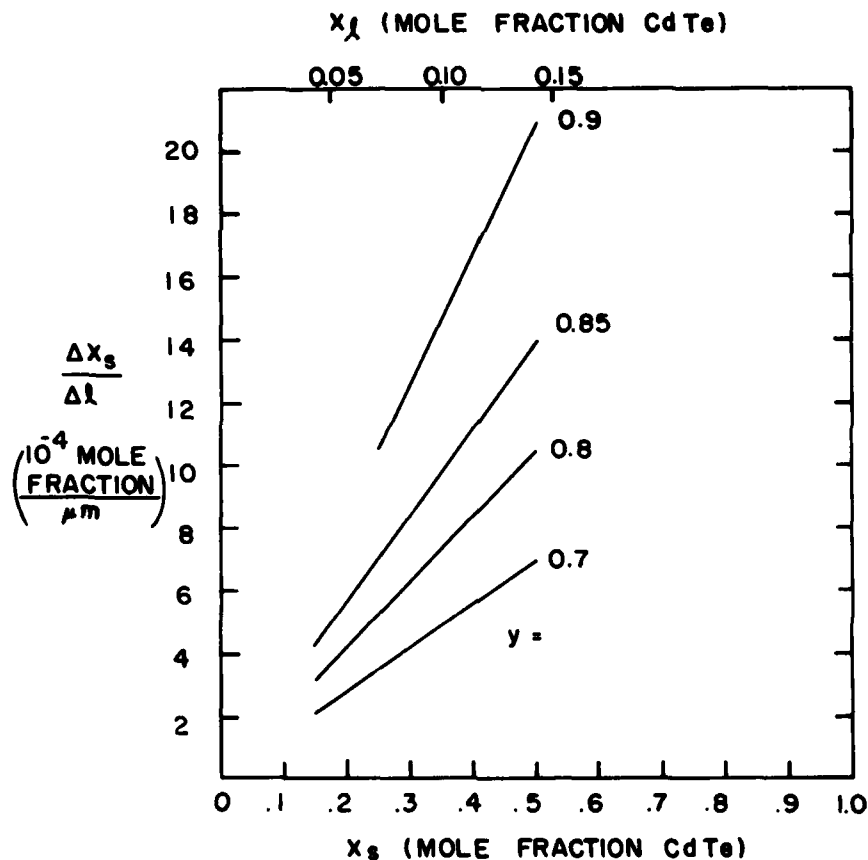


Figure 6. Change in Composition as a Function of the Layer Thickness Grown from a Solution 3mm Thick



## Section 3

### Measurement Methods

This section describes several techniques used to determine material and growth parameters. Appendices A, B, and C expand upon these and discuss additional techniques.

#### 3.1 GROWTH SOLUTION UNIFORMITY

The liquid phase epitaxial (LPE) growth of  $\text{Hg}_{1-x}\text{Cd}_x\text{Te}$  which we are pursuing is from a Te-rich solution. The composition grown and the growth temperature depend on the composition of the source solution. A typical growth solution weighs 1.5 g and contains less than 2 percent Cd. The small amount of Cd makes it impractical to weigh out all three constituents for each growth run. If the constituents were added in elemental form into an open tube system, all the Hg would be lost through vaporization before the solution was compounded. Our approach is to make a source ingot of desired composition by mixing together in a sealed quartz capsule elemental Hg, Cd, and Te. The mixture is heated above 600°C to ensure complete solution, agitated to ensure complete mixing, and quenched in water to prevent microscopic inhomogeneities. The resulting ingot contains a casting void down the center and consists of fine radial dendritic crystals. The ingot is removed from its capsule and crushed under clean conditions. Fragments of the ingot are loaded into the slider growth-well prior to each run. In order that the liquidus temperature,  $T_l$ , be the same each run and that the grown composition does not vary from run to run, it is essential that the ingot be homogeneous.

We use a broad area raster scan EDAX (energy dispersive analysis of X-rays) measurement to determine the homogeneity of the source ingot. Samples are selected from the tip, middle, and tail of each source ingot grown. These samples are epoxied to a suitable mounting block and are lapped, polished, and mounted in our SEM (Scanning Electron Microscope) for analysis. Typically, the EDAX attachment of the SEM is used to determine the local composition of a sample, but because the growth solutions are dendritic, the composition varies from Te to  $\text{Hg}_{1-x}\text{Cd}_x\text{Te}$  over distances on the order of micrometers. To avoid measuring a non-typical portion of a sample, we use a raster scan typically covering 1 mm<sup>2</sup> of sample area to determine composition. Our EDAX standards are  $(\text{Hg}_{1-x}\text{Cd}_x)_{1-y}\text{Te}_y$ , with y either 0.5 or 1 and the Cd concentration of a source ingot is usually less than 2 percent; therefore, we cannot accurately determine the composition of the source ingot using this technique. The uniformity of the Hg counts along an ingot, however, give an indication of the homogeneity of the ingot. We find that shaking a capsule just before quenching it gives adequate homogeneity.

#### 3.2 LAYER THICKNESS

Two methods are typically used to determine the thickness of the LPE layers grown. The

first measures thickness from the top surface of a layer. A chip is removed from the edge of a sample with a razor blade. The  $\text{Hg}_{1-x}\text{Cd}_x\text{Te}$  epitaxial layer has a lighter color than the CdTe substrate. Using an optical microscope at approximately 500X, the depth of focus is about 1  $\mu\text{m}$ . The difference between the microscope height when focused on the sample surface and on the interface boundary is the layer thickness. Figure 7 shows a micro-photo of such a chip on layer HCT74. The upper photo focuses on the surface of the epitaxially grown layer; the lower photo focuses on the boundary between the CdTe and the layer. The microscope has been lowered 5  $\mu\text{m}$  between the photos; therefore, the layer is 5  $\mu\text{m}$  thick.

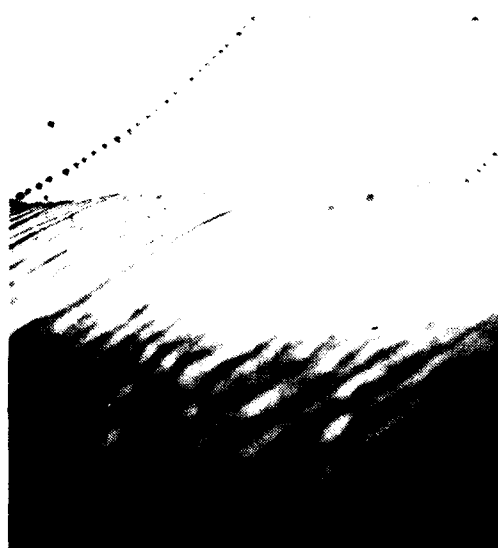
The second method provides information on the uniformity of layer thickness. For this measurement a sample is sliced from the edge of an epitaxial layer on a substrate. The sample is turned on its side, mounted in epoxy, and polished to reveal the epitaxial layer profile. The layer thickness can then be measured using a microscope or simply by using a ruler on a high magnification photograph. Figure 8 shows such a photo-micrograph of layer HCT75. This photo at 475X shows only a 200  $\mu\text{m}$  length of the 1-cm long layer. Twenty-six measurements along the length of the sample give a thickness of  $14 \pm 2 \mu\text{m}$ .

A third technique is occasionally used, but it shows surface topography rather than layer thickness. For this method we use a Talysurf Profilometer. A stylus is drawn across the surface of a sample and the relative height is recorded as a function of position. Figure 9 is an example of such a profile on layer HCT74. The features are quite prominent because of the 100-to-1 scale factor ratio for thickness compared to length. The dashed line is assumed to be the layer-substrate interface, but thickness is only determined where the layer abuts an ungrown edge. (This is the same layer shown in Figure 7.)

### 3.3 LAYER COMPOSITION

Layer composition is determined in three ways: by EDAX, by absorption measurements, and by lattice constant determination using X-rays.

Section 3.2 described a technique for measuring the layer thickness after polishing a profile. The polished edge of a layer is ideal for determining composition profiles. Using the SEM, an electron beam is focused on the sample. The beam diameter is only a fraction of a micrometer but secondary electrons cause spreading of the beam to approximately 1  $\mu\text{m}$  at a depth of several micrometers within the sample. The electrons excite the atoms in the sample. Almost instantaneously, the electrons in the excited states decay back to normal by emitting X-rays. Hg, Cd and Te and all other elements emit specific, identifiable X-ray energies. By counting the X-rays being emitted at the energies characteristics of Hg, Cd, and Te we can determine the composition of the layer. Appendix B describes the technique of comparing the count ratios with those from previously measured standards. This results in an accuracy of  $\pm 1$  mole percent in the determination of composition.



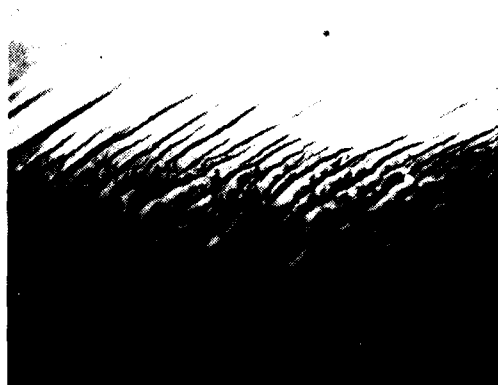
A. FOCUSED ON  
SURFACE OF LAYER

SURFACE

SLANT EDGE

Cd Te

SUBSTRATE



B. FOCUSED ON  
LAYER - SUBSTRATE  
BOUNDARY  $5\mu\text{m}$  DOWN

SURFACE

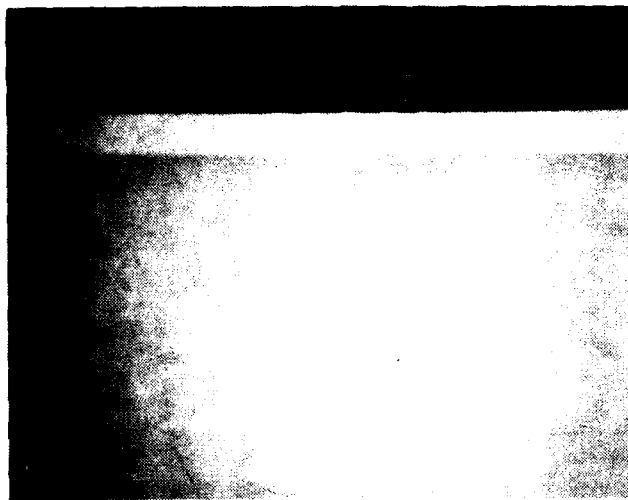
SLANT EDGE

Cd Te

SUBSTRATE

Figure 7. Two Photomicrographs of the Surface of Layer HCT74. The lower portion in the photos has been clipped off. The lateral distance between the surface and substrate is  $45\mu\text{m}$  while the layer is  $5\mu\text{m}$  thick.

HCT 75



MOUNTING EPOXY

L P E H g C d T e

Cd Te

SUBSTRATE

20  $\mu$ m

Figure 8. A Polished Cross-Section of Layer HCT75 Showing the Color Difference Between Layer and Substrate, and the Smooth Interface Boundary

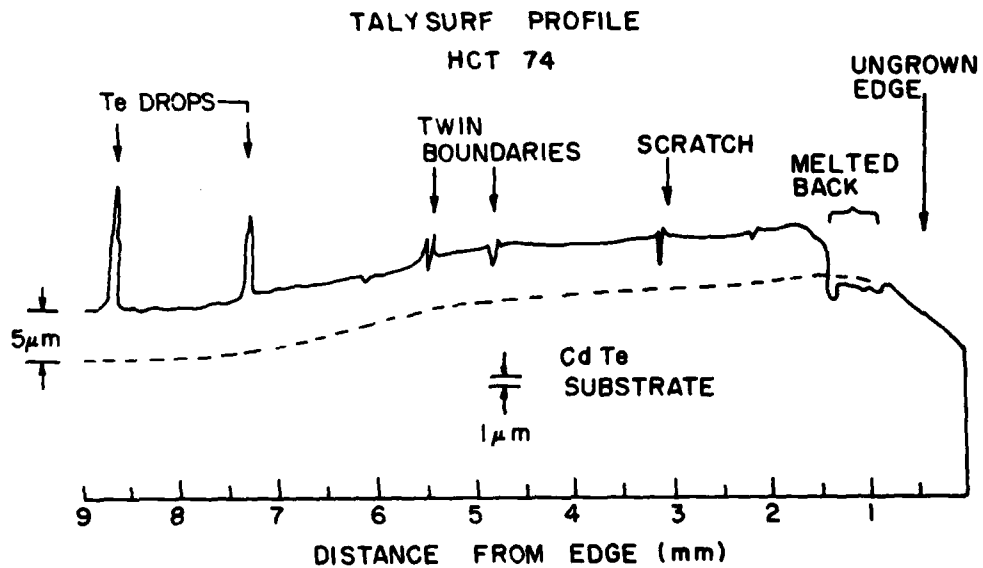


Figure 9. A Talysurf Trace of Layer HCT74 Showing the Signatures of Various Defects. The vertical scale is 100 times the horizontal scale.

The most accurate method of determining composition is to measure the transmission cutoff energy. The transmission through a sample is proportional to  $\exp(-\alpha\ell)$ , where  $\alpha$  is the absorption coefficient and  $\ell$  is the layer thickness. Because the scattering from an as grown layer is seldom predictable we do not attempt to use the absolute value of the transmission. Instead we measure the maximum transmission at an energy where the layer is transparent and calculate

$$T = T_{\text{Max}} \exp(-\alpha\ell). \quad (32)$$

If  $\ell = 500 \text{ cm}^{-1}$  is the absorption coefficient corresponding to the average gap,<sup>12</sup> then  $T$  is the transmission corresponding to the energy gap. Figure 10 shows the results of this technique with a sample  $30 \mu\text{m}$  thick having an irregular surface. From Equation 32 we find  $T_{\text{gap}} = 0.235 \exp(-500 \times 30 \times 10^{-4}) = 0.052$ .

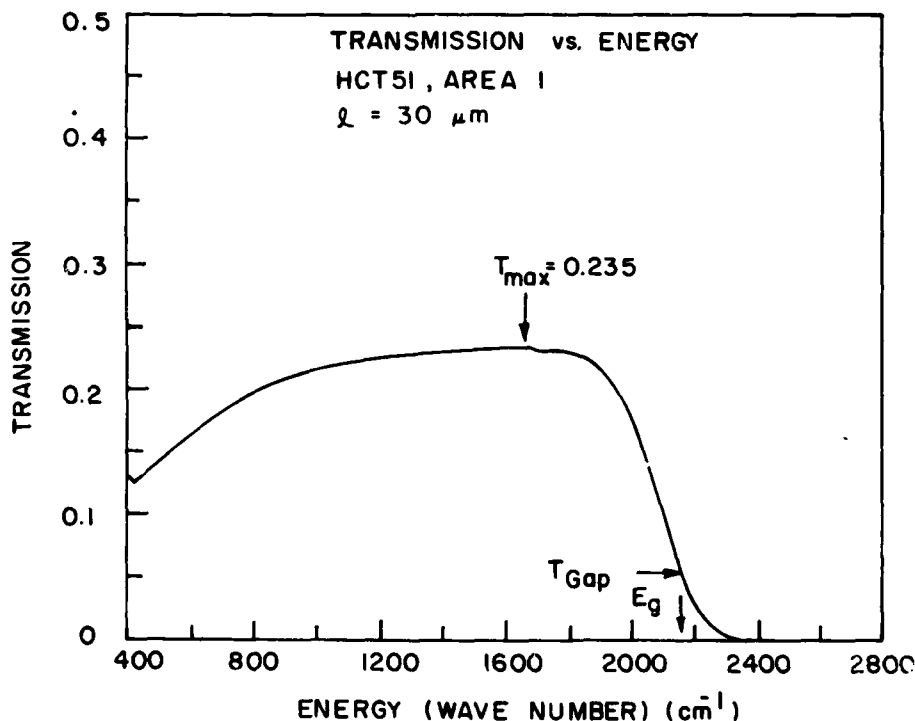


Figure 10. IR Transmission Through Layer HCT51 as a Function of Photon Energy. The energy at which the transmission drops to  $\exp(-\alpha\ell)$  of the maximum value corresponds to the energy gap.

12. M.W. Scott, *Journal of Applied Physics* 40 p. 4077, (1969).

We find  $T = 0.052$  at 2170 wave-numbers or 0.269eV. From the known dependence of energy gap on composition<sup>13</sup> we can convert the energy to  $x$ . In this case we find  $x = 0.282$ . One of the advantages of this technique is that the cutoff is sharp enough that an exact value of  $\ell$  is not needed. For example, if we used a thickness of 60  $\mu\text{m}$  instead of the correct 30  $\mu\text{m}$  value, we would get  $E_{\text{gap}} = 0.280\text{eV}$  and  $x = 0.290$ . That is, an error in  $\alpha\ell$  of a factor of 2 leads to an error in  $x$  of only about 0.01 mole fraction.

### 3.4 ELECTRICAL PROPERTIES

The main electrical properties to be measured on a layer are the carrier concentration and the mobility. For detector applications the  $R_0A$  product of diodes fabricated from a layer is also important. The Van der Pauw Hall measurements used to determine carrier concentration and mobility have been amply described in the previous interim report under this contract<sup>14</sup> and will not be repeated here. The method of measuring  $R_0A$  is also included in that report.<sup>15</sup>

Appendix A of this report includes representative Hall data taken on LPE grown material.

---

13. J.L. Schmit and E.L. Stelzer, *Journal of Applied Physics* 40 p. 4865, (1969).

14. J.L. Schmit, S.P. Tobin, and T.J. Tredwell, AFML-TR-79-4036, p. 29-36.

15. Ibid, p. 54.

## Section 4 LPE Method

### 4.1 SUBSTRATE PREPARATION

The CdTe substrates we use for the LPE growth of (Hg,Cd)Te are cut from 2-inch diameter boules supplied by II-VI Inc., Saxonburg, PA. The boules typically contain a dozen crystallites with numerous twin lines. Etching a boule for 1 second in 1:1:1 = HF:HNO<sub>3</sub>:acetic clearly reveals the twin boundaries that are in (111) planes. Careful examination of the crystallites at the surface of a boule allows one to make a reasonable guess as to which crystal dominates the bulk. Because the twin lines are in (111) planes, the orientation can be determined with the unaided eye. Orientation is confirmed using X-rays after slicing. The crystal is mounted with epoxy and sliced on a Navonic 701 ID diamond saw. CdTe is fragile and must be sliced > 1.9mm thick to prevent breakage. The crystal slices are cleaned, redipped in the 1:1:1 etch, and photographed to reveal the location of boundaries. The slices are polished to the desired thickness using a 2 percent Br in methanol solution on a lapping cloth. This chemi-mechanical polish keeps the samples flat and minimizes scratching. The finished slice is protected with a layer of beeswax and diced to the size of our slider system, either 1×1cm<sup>2</sup> or 2×3cm<sup>2</sup>. Just before use, the substrate is cleaned in hot solvents to remove the wax, given a 30-second etch in 1/2 percent Br-methanol, and rinsed in MOS grade methanol.

### 4.2 SLIDER SYSTEM

We use an atmospheric pressure growth system filled with high purity H<sub>2</sub> gas. The furnace tube is so constructed that it can be opened in a few seconds. Normally the H<sub>2</sub> is purged with high purity N<sub>2</sub> gas before opening the system. The cycle time required to open the tube, remove a grown layer, reload a new substrate and source material, and close the system is between 15 and 30 minutes. This short open time minimizes the adsorption of water on the graphite parts. Several vacuum purges and a 100°C bakeout are used to remove residual gases other than H<sub>2</sub> from the system.

The LPE slider is constructed of graphite and was machined by Poco Graphite Inc., Decatur, TX. It is basically a four-part system consisting of (1) a stationary base called a stator that contains an indent to hold the substrate, (2) a moveable portion called a slider containing wells that can be filled with growth solution, (3) a plug for the wells that minimizes Hg loss, and (4) a cover for the slider. A source of Hg is provided beneath the cover to minimize Hg loss from the growth solution. The slider is not yet perfect, and its design is still evolving.

### 4.3 GROWTH PROCEDURE

The present process in use at the Honeywell Corporate Technology Center is typically as

follows: A quartz ampule is cleaned and loaded with Te,Hg and freshly etched Cd, evaluated and sealed off. It is then slowly heated to 650°C and homogenized by rocking, held at temperature overnight, and quenched in water. The capsule is then scribed, cleaned thoroughly, and broken open. The clean source ingot is removed from the capsule, wrapped in lint-free paper, and crushed to a size that fits into the LPE slider. Samples are selected from the top, middle, and bottom of the ingot for chemical analysis to ensure that the microscopically two-phased ingot is macroscopically homogeneous. One ingot provides enough source material for a few dozen growths. Unused source ingot is stored in capped containers in a laminar flow hood to prevent contamination. For an LPE growth run, a chemi-mechanically polished and etched CdTe substrate is loaded into the stator, and 1.5 g of source ingot is loaded into a growth well in the slider. Two grams of HgTe are then loaded into the slider, which is configured so that the HgTe dissociates and provides the Hg pressure to prevent loss from the source solution. The LPE growth tube is closed, evacuated, and back filled several times with nitrogen to flush out oxygen and absorbed water and finally filled with high purity (Pd diffused) H<sub>2</sub> gas that flows at approximately 0.5 l/min. After an overnight purge, the furnace temperature is increased to above the liquidus temperature to redissolve the (Hg,Cd)Te phase in the Te phase to provide a homogeneous source solution. If insufficient time is allowed above T<sub>l</sub>, undissolved crystals will act as nucleation sites and supercooling will not be possible. The next step is to drop the furnace temperature approximately 25°C to supercool the solution, at which time the solution is slid onto the substrate. The temperature is held constant for about 30 minutes while growth occurs, after which the solution is slid off the substrate and the grown layer is cooled rapidly to room temperature. The thickness of layer grown is typically 20 μm. Note that while the furnace temperature is raised and lowered before and after growth, growth occurs from an isothermal supersaturated melt. This is important for minimizing temperature gradients and achieving layers of uniform composition.



## Section 5

### Results and Conclusions

During Phase II of F33615-77-C-5142 our goal was to demonstrate the feasibility of LPE growth of (Hg,Cd)Te from a Te-rich solution using an open-tube slider type system. We had three major accomplishments:

- Development of the open tube system
- Demonstration of the feasibility of LPE
- Communication of the results

One of the major achievements of Phase II was the design and implementation of an open-tube system to grow  $\text{Hg}_{1-x}\text{Cd}_x\text{Te}$ . This involved designing a slider system that allowed the Hg pressure to be equalized between the source solution and a HgTe supply. The design of the slider system is sufficiently unique that we have applied for a patent on it.

We can consistently grow layers with a controlled minimized Hg loss. We have demonstrated the growth of  $1\text{ cm}^2$  of  $\text{Hg}_{1-x}\text{Cd}_x\text{Te}$  having  $x = 0.2, 0.3$  and  $0.4$ , and have demonstrated the growth of  $\text{Hg}_{0.7}\text{Cd}_{0.3}\text{Te}$   $2 \times 3\text{ cm}^2$ . The composition of the grown layers is uniform both across the layers and with depth into the layers to within the precision of determining composition with the electron beam microprobe ( $\Delta x = 0.01$ ). Figure 11 shows a typical profile of composition into a layer of  $\text{Hg}_{0.6}\text{Cd}_{0.4}\text{Te}$ . Defect concentrations are low (generally fewer than 50 flaws or pinholes/ $\text{cm}^2$ ) but not yet low enough for array production. Interdiffusion with the substrate has been kept below  $3\text{ }\mu\text{m}$  by the use of a relatively low growth temperature ( $500^\circ\text{C}$ ). Figure 12 shows an SEM photo of an LPE layer of  $\text{Hg}_{0.78}\text{Cd}_{0.22}\text{Te}$   $30\text{-}\mu\text{m}$  thick showing a smooth interface region. We have also demonstrated in  $x = 0.305$  LPE grown material the fabrication of diodes having  $R_0A > 1000\text{ }\Omega\text{ cm}^2$  at  $100\text{K}$  as shown in Figure 13. These diodes were fabricated and evaluated under a different contract<sup>(16)</sup> but the results are included here for completeness. Figure 12 shows the two best diodes made from LPE layer HCT41. The data points taken at room temperature have been deleted because the resistance is dominated by series resistance. The acceptor concentration measured by Van der Pauw Hall was  $1.2 \times 10^{17}\text{ cm}^{-3}$  and the composition determined by measuring the transmission cut-off edge is  $\text{Hg}_{0.695}\text{Cd}_{0.305}\text{Te}$ . The straight lines in Figure 13 are arbitrary in magnitude and have slopes proportional to  $1/n_i$  (as does gr limited current) and to  $1/n_i^2$  (as does diffusion limited current). These are the first diodes we have made on our LPE grown material and the carrier concentration is not optimum; therefore, we cannot draw any firm conclusions. However, these particular diodes appear to be diffusion current limited down to approximately  $100\text{K}$  and could be shunt current limited at lower temperatures.

---

16. P. LoVecchio, Contract F33615-78-C-5156.

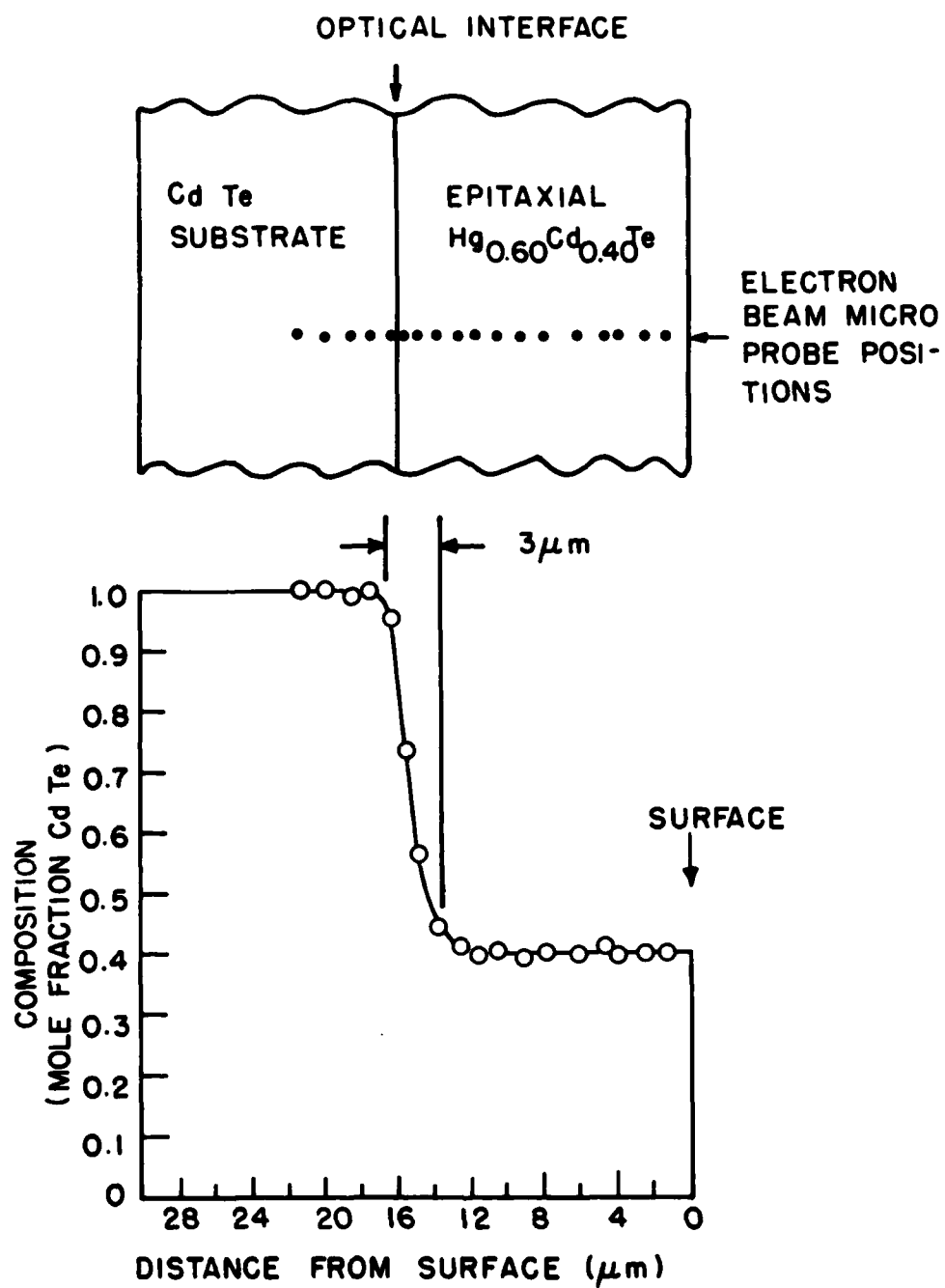


Figure 11. Variation of CdTe Mole Fraction With Depth Into an LPE Layer



Figure 12. SEM Profile of an LPE Layer

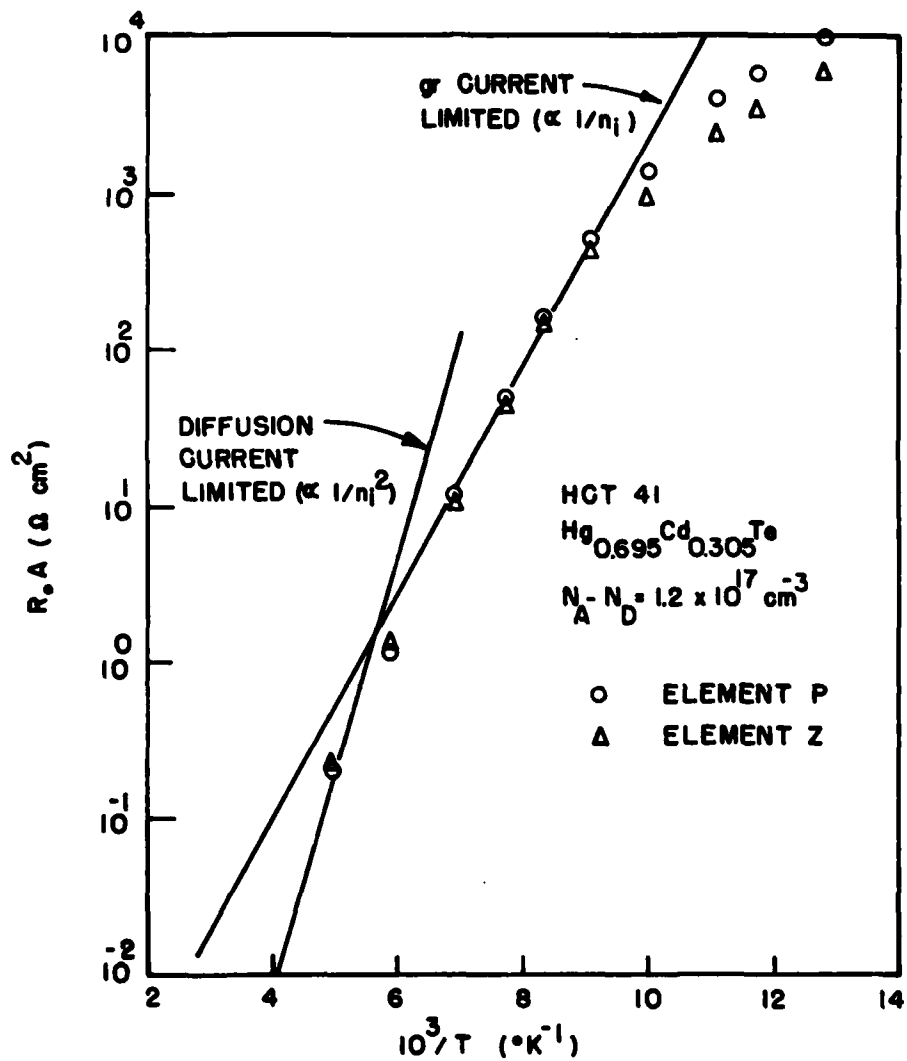


Figure 13.  $R_o A_j$  for 2 Diodes Made from  $\text{Hg}_{0.695}\text{Cd}_{0.305}\text{Te}$  Layer HCT41

These results have been communicated in three publications this year. The first, included as Appendix A, was published in *Applied Physics Letters* and it reports on the compositional uniformity and the electrical properties of LPE grown layers of  $\text{Hg}_{0.6}\text{Cd}_{0.4}\text{Te}$  grown from Te-rich solution. The second, included as Appendix B, was given at the IRIS-DSGM in June and will be published in the IRIS proceedings sometimes later. It describes the characterization techniques used to determine tie lines, composition, and electrical properties. The third, included as Appendix C, has been published in the *IEEE Transactions on Electron Devices*, January 1980, a special issue on infrared. It compares LPE layers grown from Te-rich solution at atmospheric pressure in our present slider system with material grown from Hg-rich solution in a sealed tube and with material grown from a HgTe-rich solution in a sealed tube. The interdiffusion depth was found to be mainly dependent on growth temperature.

A few tie lines of practical importance have been determined but have not yet been published. The liquidus temperatures were determined by doing LPE growths at successively higher temperatures until melt-back occurred instead of growth. The liquidus composition was assumed to be the loaded composition and the solid composition was determined by use of electron beam microprobe and by optical transmission cut-off energy, as described in Appendix B. The five tie lines determined under this contract are listed in Table 4.

Table 4. Tie Line Parameters

Source Solution			Solid Grown	Ratio, k
x	y	$T_\ell$	x	$x_s/x_\ell$
0.1	0.825	508°C	0.40	4.00
0.095	0.82	508°C	0.37	3.89
0.082	0.81	507°C	0.29	3.54
0.06	0.80	510°C	0.22	3.67
0.05	0.80	499°C	0.195	3.90

The ratio of  $x_{\text{solid}}/x_{\text{liquid}}$  is defined as the segregation coefficient, k. The k values from these data were included in Figure 2 along with k values taken from the pseudo-binary ( $y = 0.5$ ) phase diagram. Our assumption that k is independent of y is seen to be generally true, but the inverted curvature is disconcerting. The compositions grown are accurately known, but the compositions of the solutions could be in error due to Hg loss before growth began. It seems unlikely that random Hg loss would yield such a smoothly varying function. Next year we will determine k for  $x_s \approx 0.8$  and determine if the trend continues.

During the course of the contract we have done 100 growth runs. Many of them have been used to determine liquidus temperature or Hg loss from the growth solution and did not result in a layer to be evaluated. This contract has resulted in the demonstration of feasibility and it is not possible to detail all the steps along the way. We have used growth temperatures between 450 and 515°C and find the most important factor is that growth occur not more than 10°C below the liquidus temperature. Excessive supercooling leads to precipitation within the solution, not just on the substrate.

We have checked the orientation of substrate and layer for several runs and find that epitaxy always occurs. Even when a polycrystalline substrate was used the layer replicated all orientations.

We have grown layers mainly on (111)A and (111)B substrates but have also grown a few on (110) and (100) CdTe. To a first approximation we found no difference between the different major orientations, but growth more than a degree off a major direction leads to line defects. The (111)A and (111)B orientations are greatly preferred because twin boundaries occur in the (111) planes of CdTe so that (111) plane slices do not intercept the twin lines. Most of these comparisons were done early in the year before the technique was perfected so that they have limited validity. The (111)A face is currently preferred.

Thickness of the layers grown falls into 3 groups. 1) Layers are from 2- to 5- $\mu\text{m}$  thick if they are grown from a solution with excessive supercooling. The spontaneous precipitation throughout the melt means the solution is never supersaturated, so growth is minimal. 2) A layer thickness of 15 to 25  $\mu\text{m}$  occurs with a super cooling of approximately 5°C. This is in essential agreement with the thickness predicted in Section 2. Figure 5 predicts a layer thickness of between 4 and 5  $\mu\text{m}/^\circ\text{C}$  for solutions having  $y = 0.8$  and  $x_s$  between 0.2 and 0.4. 3) We grew a few layers having a thickness between 31 and 54  $\mu\text{m}$  by the expedient of slowly programming the temperature down during growth. For example, layer HCT 95 was cooled 28°C during growth and was 54  $\mu\text{m}$  thick. Figure 5 predicts approximately 100- $\mu\text{m}$  thick growth, so we assume that complete mixing did not occur in this case. In general, the layer quality improves with thickness. The layers < 5  $\mu\text{m}$  thick have a pinhole density >  $10^3\text{cm}^{-2}$ , while those > 20  $\mu\text{m}$  thick have fewer than 50 defects per  $\text{cm}^2$ . This could be the result of the different growth mechanism mentioned above.

Most of the layers grown have been 1  $\text{cm}^2$ ; however, several have been grown with dimensions of  $2 \times 3 \text{ cm}^2$ . We have demonstrated that the technique is relatively easy to scale in size. The next step is to fine tune the control of the growth parameters so that high quality layers can be grown consistently.

## References

1. J.P. Schwartz, Ph.D. Thesis, Marquette University, p. 99 (1977).
2. W. Jost, *Diffusion in Solids, Liquids and Gases*, Academic Press, NY (1952).
3. J.A. Mroczkowski, Contract F33615-78-C-5156, Letter Report 11 (July-August, 1979).
4. Ted Harman of MIT Lincoln Labs, private communication.
5. T.C. Harman and A.J. Strauss, *Physics and Chemistry of II-VI Compounds*, Interscience, p. 784 (1967).
6. J. Steininger, *Journal of Electronic Materials* 5, pp. 299-320 (1976).
7. J. Blair and R. Newnham, *Metallurgy of Elemental and Compound Semiconductors*, Interscience 12, p. 393 (1961).
8. J.L. Schmit and M.W. Scott, unpublished results.
9. J.E. Bowers, J.L. Schmit, and J.A. Mroczkowski, "Characterization of LPE Grown  $\text{Hg}_{1-x}\text{Cd}_x\text{Te}$ ," IRIS Detector Specialty Group Meeting (June 1979), Minneapolis, MN, Figure 3. (Also see Appendix B.)
10. D. Long and J.L. Schmit, *Semiconductors and Semimetals*, Academic Press, 5, Chapter 5, p. 243 (1970).
11. Bruce Chalmers, *Physical Metallurgy*, John Wiley and Sons, p. 79 (1959).
12. M.W. Scott, *Journal of Applied Physics* 40, p. 4077 (1969).
13. J.L. Schmit and E.L. Stelzer, *Journal of Applied Physics* 40, p. 4865 (1969).
14. J.L. Schmit, S.P. Tobin, and T.J. Tredwell, AFML-TR-79-4036, pp. 29-36.
15. Ibid, p. 54.
16. P. LoVecchio, Contract F33615-78-C-5156.

## **Appendices**

Many of the results of AFML Contract F33615-77-C-5142 relevant to LPE growth of HgCdTe have already been submitted for publication, but have not yet appeared in print. In this section, we reproduce those papers to make them available to the reader.



**Appendix A**  
**LPE Growth of  $\text{Hg}_{0.60}\text{Cd}_{0.40}\text{Te}$  from Te-rich Solution**

Joseph L. Schmit and John E. Bowers, published in Appl. Phys. Lett. **35**, 457-458 (1979).

## LPE growth of $\text{Hg}_{0.60}\text{Cd}_{0.40}\text{Te}$ from Te-rich solution

Joseph L. Schmit and John E. Bowers

Honeywell Corporate Technology Center, Bloomington, Minnesota 55420

(Received 23 April 1979; accepted for publication 2 July 1979)

$\text{Hg}_{0.60}\text{Cd}_{0.40}\text{Te}$  has been grown at atmospheric pressure using a liquid phase epitaxy (LPE) slider system. The compositions are uniform to within  $\pm 0.01$  mole fraction across the layer and with depth into the layer except for a  $3\text{-}\mu\text{m}$ -thick interdiffusion region. The layers are  $p$  type as grown with carrier concentration of  $10^{17}\text{ cm}^{-3}$  and are annealable to  $n$  type with a carrier concentration of  $4 \times 10^{15}\text{ cm}^{-3}$ .

PACS numbers: 81.10.Dn

LPE growth techniques can satisfy the needs of advanced intrinsic infrared focal planes for large-area  $\text{HgCdTe}$  with good control of composition and doping levels. Multi-layer growth is advantageous for the fabrication of both monolithic  $\text{HgCdTe}$  detectors and CCD's and hybrid devices using  $\text{HgCdTe}$  detectors mated to silicon CCD's.

$\text{HgCdTe}$  has been grown by LPE from solutions of  $\text{Hg}$ ,<sup>1</sup> from  $\text{HgTe}$  (along the  $\text{HgTe}$ - $\text{CdTe}$  pseudobinary),<sup>2</sup> and from Te solution.<sup>3,4</sup> For growth from  $\text{Hg}$  solution, the  $\text{Hg}$  pressure is typically 8 atm for growth temperatures of about  $500^\circ\text{C}$  which prohibits open tube growth. The  $\text{Hg}$  pressure can be lowered by lowering the growth temperature, but temperatures below  $240^\circ\text{C}$  must be used to keep the pressure below 0.1 atm. For growth anywhere along the pseudobinary, the pressure is above 10 atm. For growth from a Te-rich solution, the  $\text{Hg}$  pressure can be kept below 0.1 atm for growth temperatures below  $500^\circ\text{C}$ .<sup>5</sup> This low pressure makes open-tube slider growth possible. Recently, Harman<sup>6</sup> and Lanir *et*

*al.*<sup>7</sup> have reported LPE growth of  $\text{HgCdTe}$  from Te-rich solutions. Details of the composition, compositional uniformity of the alloy, or characteristics of their layers after annealing were not presented.

In this paper we present the results of LPE crystal growth experiments using an open-tube slider apparatus. The layers were grown with a composition of  $\text{Hg}_{0.60}\text{Cd}_{0.40}\text{Te}$  on  $\text{CdTe}$  substrates. The compositional uniformity of the layers has been measured, as well as the electrical characteristics of annealed layers.

The growths were done using a horizontal slider-type graphite boat. The boat is contained in a quartz tube leak checked to  $10^{-7}$  Torr and back filled with high-purity Pd-diffused hydrogen flowing at  $\sim 500\text{ cc/min}$ . Substrates were chemimechanically polished (111)*A* and (111)*B* faces of  $\text{CdTe}$  of area  $1\text{ cm}^2$ . A solution of  $(\text{Hg}_{0.9}\text{Cd}_{0.1})_{0.175}\text{Te}_{0.825}$  was homogenized for 30 min  $\sim 25^\circ\text{C}$  above the liquidus temperature just prior to growth for  $\sim 30\text{ min}$  at  $500^\circ\text{C}$ . The resulting layer was cooled quickly to room temperature to minimize interdiffusion after growth.

The epitaxial layers grown were microscopically smooth with occasional defects. Meniscus lines and terracing were rarely observed. The pinhole densities were usually less than  $100/\text{cm}^2$  in layers  $16\text{ }\mu\text{m}$  thick. The composition of grown layers was determined with an SEM using energy dispersive analysis of x-rays (EDAX) by comparing the x-ray emission from the layers to reference samples whose composition was determined by density measurements. The experimental error in the EDAX measurements is  $\pm 0.01$  mole fraction  $\text{CdTe}$ . The carrier concentrations and mobility val-

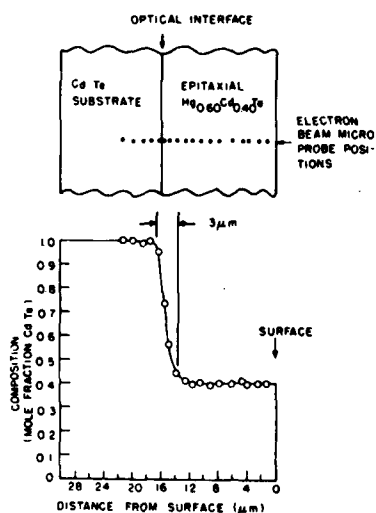


FIG. 1. Variation of mole fraction  $\text{CdTe}$  with depth into the layer.

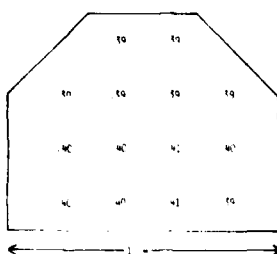


FIG. 2. Variation of mole fraction  $\text{CdTe}$  across an epitaxial layer.

TABLE I. Electrical characteristics of epitaxial-grown and bulk-grown  $\text{Hg}_{0.40}\text{Cd}_{0.60}\text{Te}$  (Ref. 7).

	Epitaxial layer (as-grown)	Bulk ( $Q/A$ ) (500 °C Te- rich anneal)	Epitaxial layer (300 °C Hg- rich anneal)	Bulk ( $Q/A$ ) (300 °C Hg- rich anneal)
Type	$p$	$p$	$n$	$n$
Carrier concentration ( $\text{cm}^{-3}$ )	$1 \times 10^{11}$	$2 \times 10^{11}$	$4 \times 10^{11}$	$5 \times 10^{11}$
Mobility ( $\text{cm}^2/\text{Vs}$ )	300 °K 96	100	1430	4500
	77 °K 220	300	4660	20 000
Activation energy (eV)	0.0013	0.002	...	0

ues were determined using van der Pauw Hall coefficient measurements.

The layer compositions were  $x = 0.40$  with run-to-run variations in composition of 0.02. The lattice constant was measured using x-ray techniques to be 6.46 Å, which corresponds to a composition<sup>6</sup> of  $x = 0.39$ , in agreement with the EDAX measurement. The variation of composition with depth is shown in Fig. 1. The composition is constant over 14  $\mu\text{m}$  of the epitaxial layer, then varies from  $x = 0.4$  to  $x = 1.0$  in  $\sim 4 \mu\text{m}$ . The variation in composition across the surface of the layer is within  $\pm 0.01$  mole fraction CdTe (see Fig. 2).

The carrier concentration and mobility of an as-grown layer are given in the first column of Table I. The results for a bulk-grown sample annealed in saturated Te vapor at our growth temperature (see second column, Table I) are similar to the LPE layer results. Schmit and Stelzer<sup>7</sup> found that annealing in saturated Hg vapor at 300 °C converted bulk-grown samples to  $n$  type with high mobility (see fourth column, Table I). Using this anneal, the epitaxial layer converted to  $n$  type with a carrier concentration of  $4 \times 10^{11} \text{ cm}^{-3}$  (see third column, Table I). For the as-grown  $p$ -type LPE layer, the carrier concentration is limited by stoichiometric defects and the mobility at 77 °K is limited by ionized impurity scattering.<sup>8</sup> We believe that the carrier concentration after annealing is limited by residual donor impurities as was found to be the case in bulk-grown material.<sup>7</sup> The lattice-scattering-limited mobility for this composition at 77 °K is  $2 \times 10^4 \text{ cm}^2/\text{Vs}$ .<sup>9</sup> Either strain or ionized impurity scattering due to

compensation could be limiting the LPE layer mobility after annealing to less than  $5000 \text{ cm}^2/\text{Vs}$ . The acceptor activation energy can be determined from the temperature dependence of the Hall coefficient below 77 °K.<sup>10</sup> We find a very small activation energy for the LPE sample just as was found earlier for the bulk-grown samples of similar concentration.

In conclusion, we have grown  $\text{Hg}_{0.40}\text{Cd}_{0.60}\text{Te}$  layers uniform to within  $\pm 0.01$  mole fraction with good surface morphology and electrical properties comparable to bulk-grown  $n$ -type crystals. The layers can be converted to  $n$  type with carrier concentration of  $4 \times 10^{11} \text{ cm}^{-3}$  and 77 °K mobility of  $4660 \text{ cm}^2/\text{Vs}$ .

The authors thank D. George for making the EDAX measurements and W. Scott, E. Johnson, and R. Engh for helpful discussions. This work was partially supported by the Air Force Materials Laboratory under contract F33615-77-C-5142, monitored by R. Hickmott.

<sup>1</sup>R. Macielek (private communication).

<sup>2</sup>C. Speerschender (private communication).

<sup>3</sup>T.C. Harman, *J. Electron. Mater.* 8, 191 (1979).

<sup>4</sup>M. Lanir, C.C. Wang, and A.H.B. van der Wyck, *Appl. Phys. Lett.* 34, 50 (1979).

<sup>5</sup>J.P. Schwartz, Ph.D. thesis, Marquette Univ., 1977, p. 99.

<sup>6</sup>J.C. Woolley and B. Ray, *J. Phys. Chem. Solids* 13, 151 (1960).

<sup>7</sup>J.L. Schmit and E.L. Stelzer, *J. Electron. Mater.* 7, 65 (1978).

<sup>8</sup>W. Scott, E.L. Stelzer, and R.J. Hager, *J. Appl. Phys.* 47, 1408 (1976).

<sup>9</sup>W. Scott, *J. Appl. Phys.* 43, 1055 (1972).

<sup>10</sup>J.S. Blakemore, *Electron. Commun.* 29, 131 (1952).

## **APPENDIX B**

### **CHARACTERIZATION OF LPE GROWN $\text{Hg}_{1-x}\text{Cd}_x\text{Te}$**

J. E. Bowers, J. L. Schmit and J. A. Mroczkowski, Presented at the 1979 Detector Specialty Meeting of IRIS and to be published in the IRIS proceedings in late 1979.

#### **CHARACTERIZATION OF LPE GROWN $\text{Hg}_{1-x}\text{Cd}_x\text{Te}$**

**June 1, 1979**

**J. E. Bowers and J. L. Schmit  
Honeywell Corporate Technology Center  
Bloomington, MN 55420**

**and**

**J. A. Mroczkowski  
Honeywell ElectroOptics Center  
Lexington, MA 02173**

## Abstract

$\text{Hg}_{1-x}\text{Cd}_x\text{Te}$  has been grown from Te-rich solution at atmospheric pressure using a liquid phase epitaxy (LPE) slider type system and in sealed quartz ampules using a tipping technique. The layers are p-type as grown with  $\sim 10^{17} \text{ cm}^{-3}$  acceptors and can be annealed to  $4 \times 10^{15} \text{ cm}^{-3}$  donors. The layers have composition constant to  $\pm 1$  mole percent across the layer and with depth into the layer. Composition is determined by EDAX and confirmed by measurement of the lattice constant using x-rays and by the cut-off wave-length of transmission. Preliminary measurements of minority carrier lifetime on LPE grown material show lifetime several times longer than for bulk-grown material.

## 1. INTRODUCTION

$\text{Hg}_{1-x}\text{Cd}_x\text{Te}$  has proven to be a versatile and reliable semiconductor for use in ir detectors. In recent years its success has led to more widespread use and to more sophisticated array designs. Current applications for use in focal planes require hundreds of elements per array, and the need to reduce costs dictates that many arrays be fabricated simultaneously. Liquid phase epitaxy (LPE) has been used extensively for the growth of large area III-V compounds and several people have reported on the growth of  $\text{Hg}_{1-x}\text{Cd}_x\text{Te}$  using LPE.<sup>1-4</sup>

In this paper we report the techniques we use to determine liquidus temperatures, surface morphology, composition and minority carrier lifetime. We give the liquidus temperatures of several Te-rich solutions, give tie-lines for four compositions of interest and describe two LPE growth systems which were used. We report the growth of  $\text{Hg}_{1-x}\text{Cd}_x\text{Te}$  layers having  $0.2 < x < 0.4$  from Te-rich solutions and describe their growth morphology, composition uniformity, and carrier concentrations.

## 2. EXPERIMENTAL TECHNIQUES

### Liquidus Temperature:

The approximate liquidus temperatures of Te-rich solutions were obtained by differential thermal analysis (DTA). These compositions exhibited random supercooling of at least 2 to 15°C. The best estimate of the liquidus temperature was obtained for each composition by extrapolation from a plot of degree of supercooling versus the temperature at which the supercooling stopped. At least eight cooling runs were used for each composition. The amplitude of the differential temperature overshoot was used as a measure of the degree of supercooling.

A more precise liquidus temperature was determined for some compositions by doing isothermal LPE growths at several temperatures and observing the transition from melt-back to growth.

#### **Growth:**

Two LPE systems have been used to grow the layers reported in this paper. At Honeywell we have been growing  $\text{Hg}_{1-x}\text{Cd}_x\text{Te}$  by LPE since 1971.<sup>5</sup> Most of the growths have been from HgTe-rich solutions along the pseudobinary at  $\sim 700^\circ\text{C}$ . This high growth temperature causes a Hg pressure of several atmospheres. A closed-tube tipping-type system was developed to grow at those pressures<sup>6</sup> and has been used for the initial growths from Te-rich solutions. This system pours liquid Te-rich solution onto a  $1 \times 4 \text{ cm}^2$  substrate configured such that the solution is of uniform depth over the substrate. The temperature is lowered at less than  $1^\circ\text{C}$  per minute, and the solution is poured off after growing a layer.

In the fall of 1978 an open-tube slider-type system was designed and built. The open tube design was made possible by the lower Hg vapor pressure over Te-rich solution<sup>7</sup> and permits operating the slider using external push rods. The slider makes it possible to grow multiple layers of different composition sequentially. The low Hg vapor pressure allows the growth of large area layers although single crystal CdTe substrates more than 3 cm in diameter are not readily available. Our graphite slider is machined to grow either  $1 \times 1 \text{ cm}^2$  or  $2 \times 3 \text{ cm}^2$  layers.

#### **Morphology:**

Growth morphology was determined qualitatively by observing specular reflection and quantitatively by using a Nomarski phase contrast microscope. Pinholes are counted on representative areas of a wafer except for low-density wafers for which the entire wafer was counted. Depth of surface defects was determined by two techniques. A Taylor-Hobson Talystep 1 instrument for measuring film thickness traverses a stylus across the surface of a sample and registers relative height to  $0.1 \mu\text{m}$ . The phase contrast microscope at  $\sim 500\times$  magnification has a depth of focus of  $\sim 1 \mu\text{m}$  so it is also used to determine the depth of defects. Normally the corners of a wafer are left ungrown to act as a reference to measure the thickness of the grown layer. A more accurate determination of thickness is made by polishing a cross section and using a scanning electron microscope (SEM) to make a high magnification photo. Thickness and uniformity of thickness can then be measured with a ruler. Normally the composition is also measured while the sample is in the SEM. We find that the apparent boundary between the substrate and the grown layer of  $\text{Hg}_{1-x}\text{Cd}_x\text{Te}$  occurs at  $x \approx 0.8$ .

### Composition:

Composition of bulk  $\text{Hg}_{1-x}\text{Cd}_x\text{Te}$  is usually determined by measuring the density, but such a technique is not suitable for thin LPE layers. We typically use the EDAX (Energy Dispersive Analysis of X-rays) attachment to our SEM to determine composition. This instrument is usually used as a qualitative measure of elements present, but with the addition of a set of standards, it gives quantitative results with a precision of one mole percent. Figure 1 is plot of the Hg and Cd counts normalized to 8000 Te counts for the 10 standards we have. The composition of the standards was determined by density measurements. Composition is determined from both Hg counts and Cd counts and the results averaged if there is any difference. The spatial resolution of the SEM permits determination of composition on areas as small as  $1\text{ }\mu\text{m}$  across. EDAX measures only the surface few micrometers, therefore samples must be prepared properly to assure that the surface is representative of the layer grown. The last step we use before EDAX is a polish with  $0.3\text{ }\mu\text{m}$  grit. Etches can change surface composition.

The composition as measured by EDAX was checked by measuring the lattice constant using a Bond x-ray diffractometer and the  $\text{Cu K}\alpha$  line. The composition of  $\text{Hg}_{1-x}\text{Cd}_x\text{Te}$  can be determined directly since the lattice constant varies linearly with composition.<sup>8</sup> This technique gives only the average composition of a layer with a precision of  $\pm 2$  mole percent.

Composition is also determined from the energy gap. The energy corresponding to an absorption coefficient of  $500\text{cm}^{-1}$  is assumed to be the energy gap.<sup>9</sup> The assumption does not limit our accuracy since the transmission cut-off is sharp (40% to 5% transmission in 50 wave numbers or 0.006 eV). The composition is determined from the energy gap using the empirical expression of Schmit & Stelzer.<sup>10</sup> The transmission technique is the most reliable for determining average lowest composition of a single layer, but cannot be easily used for multilayer samples or very small areas.

### Lifetime:

Minority carrier lifetime is measured using the reverse recovery technique.<sup>11</sup> Figure 2 shows a schematic of the circuit and a typical scope tracing to determine the switching time. Several different interpretations of the data are possible<sup>12</sup> but the simplest is that due to Kingston<sup>11</sup> who assumes an abrupt junction and a depletion width greater than the diffusion length. His expression is:

$$\text{erf} \sqrt{\frac{t_s}{\tau_e}} = \frac{1}{1 + \frac{I_R}{I_F}}$$

where  $t_s$  = Switching time  
 $\tau_e$  = Minority carrier lifetime  
 $I_R$  = Reverse Current  
 $I_F$  = Forward Current

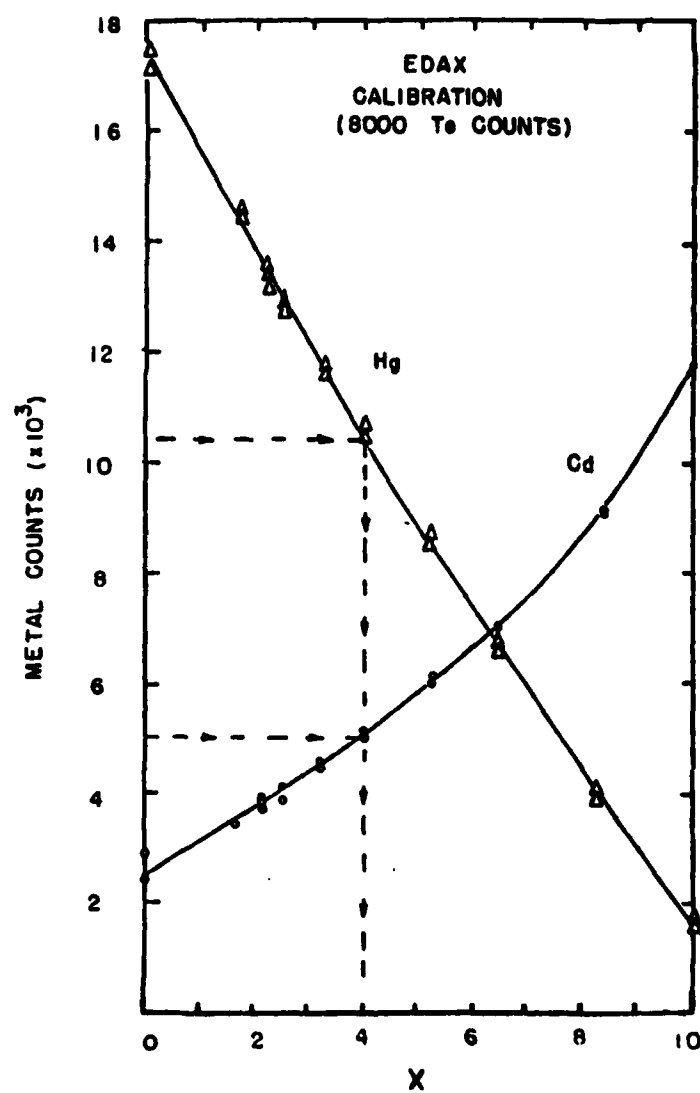


Figure 1. EDAX Calibration. Mercury and cadmium counts on 10 samples as a function of composition.



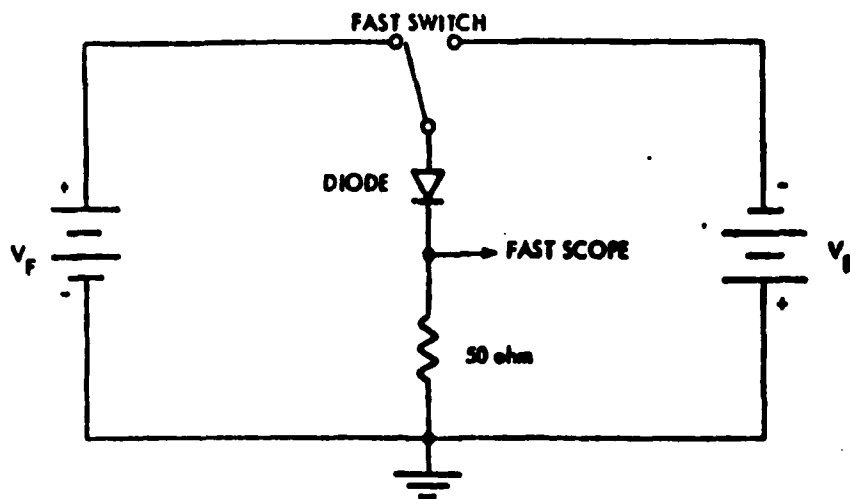


Figure 2a. Schematic Diagram of Reverse Recovery Circuit.

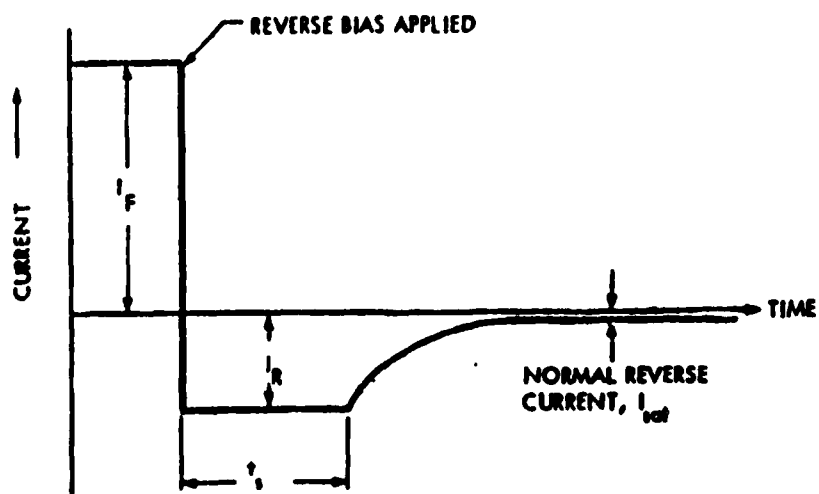


Figure 2b. Current vs. Time Measured in Reverse Recovery

This technique oversimplifies the problem but provides data on  $\tau_e$  within a factor of two<sup>12</sup> of the more rigorous Kuno technique<sup>13</sup>, and is useful for comparing material prepared by different methods, such as quench-anneal and LPE.

### 3. RESULTS AND DISCUSSION

Figure 3 is a plot of liquidus temperatures of Te-rich  $(\text{Hg}_{1-x}\text{Cd}_x\text{Te})_{1-y}\text{Te}_y$ . The lower curve is for HgTe from the data of Brebrick and Strauss.<sup>14</sup> The two upper curves are for  $x = 0.067$  and  $x = 0.10$ . Liquidus temperatures are those at which solute begins to freeze out upon cooling. Figure 3 gives some liquidus temperatures but does not define the solid compositions in equilibrium at each. Figure 4 is a plot of the Te-pseudobinary quadrant of the Hg-Cd-Te ternary phase diagram. It shows the liquidus temperature data from the previous figure along with four tie-lines connecting liquid compositions with the solid  $\text{Hg}_{1-x}\text{Cd}_x\text{Te}$  composition which grows from each. These were determined by growing LPE layers from solutions of known composition and determining the compositions of the resulting layers.

As mentioned earlier, EDAX is our prime technique for determining composition. Table 1 compares the composition of three layers grown from identical solutions and measured by three techniques.

We find agreement within experimental error among the three techniques. Figure 5 is a plot of transmission as a function of energy using an FTS spectrometer. This layer was  $13\mu\text{m}$  thick so  $\alpha = 500$  corresponds to 23% transmission. This occurs at  $2950\text{cm}^{-1}$  or  $0.366\text{eV}$  corresponding to  $x = 0.38$  at  $6.5\text{K}$ .<sup>10</sup> We also checked this sample at room temperature and deduced  $x = 0.38$  although the cutoff was not quite as sharp. For the determination of lattice constant on growth run 25, we measured  $6.483\text{\AA}$  for the CdTe substrate in agreement with accepted values.<sup>8, 15</sup> for the grown layer we found a lattice constant of  $6.469 \pm .0005\text{ \AA}$  which corresponds to  $x = 0.39 \pm .02$ .

Most samples have composition determined only by EDAX. Figure 6 gives the composition of a  $2 \times 3\text{ cm}^2$  layer grown by open tube slider LPE from Te-rich solution at  $500^\circ\text{C}$ . The composition is  $0.34 \pm .01$  which is within the experimental accuracy of the EDAX. Composition of a  $1 \times 1\text{ cm}^2$  layer grown from a different solution at  $500^\circ\text{C}$  was  $0.40 \pm .01$ . Thus we have good surface uniformity for both large and small layers. Figure 7 gives composition as a function of depth into a layer. For comparison, the profile of a typical layer grown from HgTe-rich solution at  $700^\circ\text{C}$  is also included. The minimal inter-diffusion occurring at the  $500^\circ\text{C}$  growth temperature is apparent. Figure 8 shows the compositional profile of a double epitaxial layer. These layers were grown one immediately after the other by sliding a second solution over the substrate without changing the temperature. Note that the top layer has a higher composition than the first layer. With LPE the growth temperature is considerably below the solidus temperature so growth can be either from high to low  $x$  as for the first layer, or from low to high  $x$  as with the second layer.

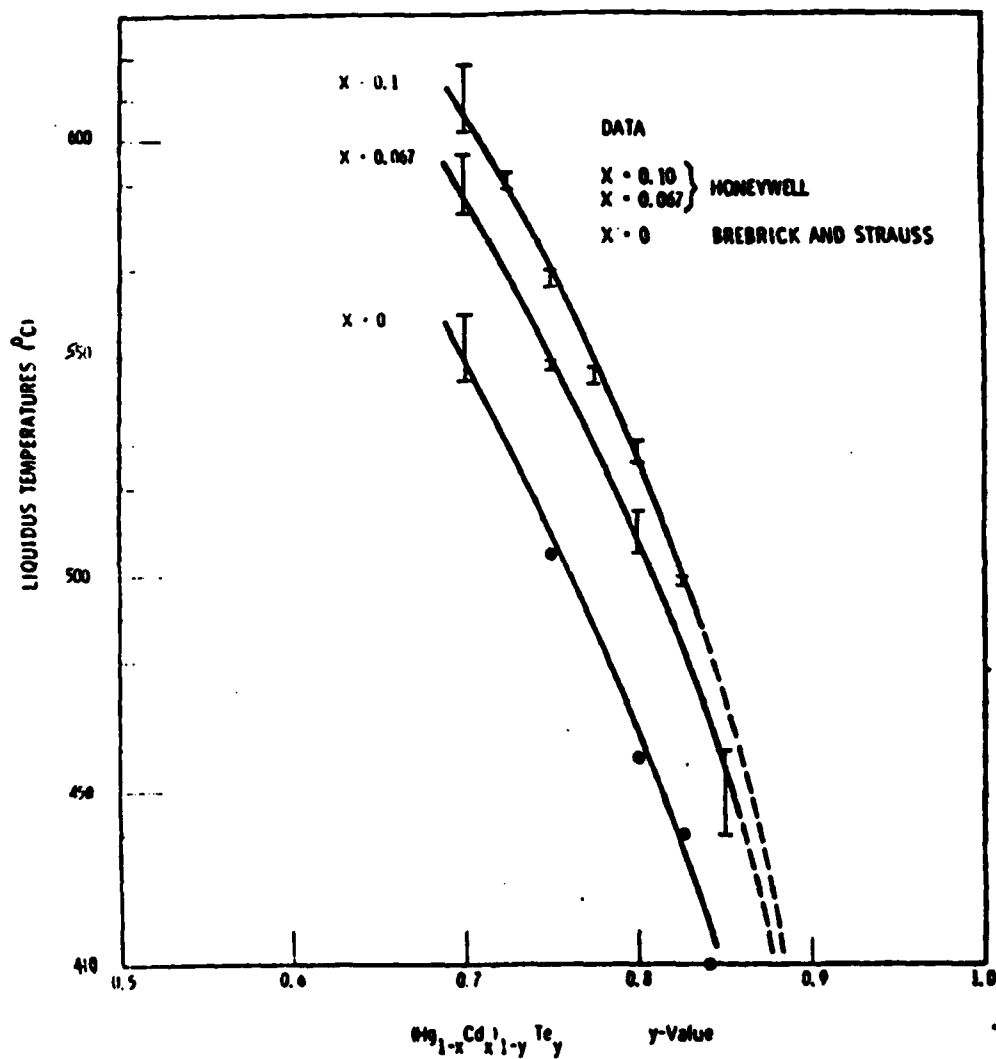


Figure 3. Liquidus Temperature. Liquidus temperature of  $(\text{Hg}_{1-x}\text{Cd}_x)_{1-y}\text{Te}_y$  as a function of Te-fraction, y, for three values of x.

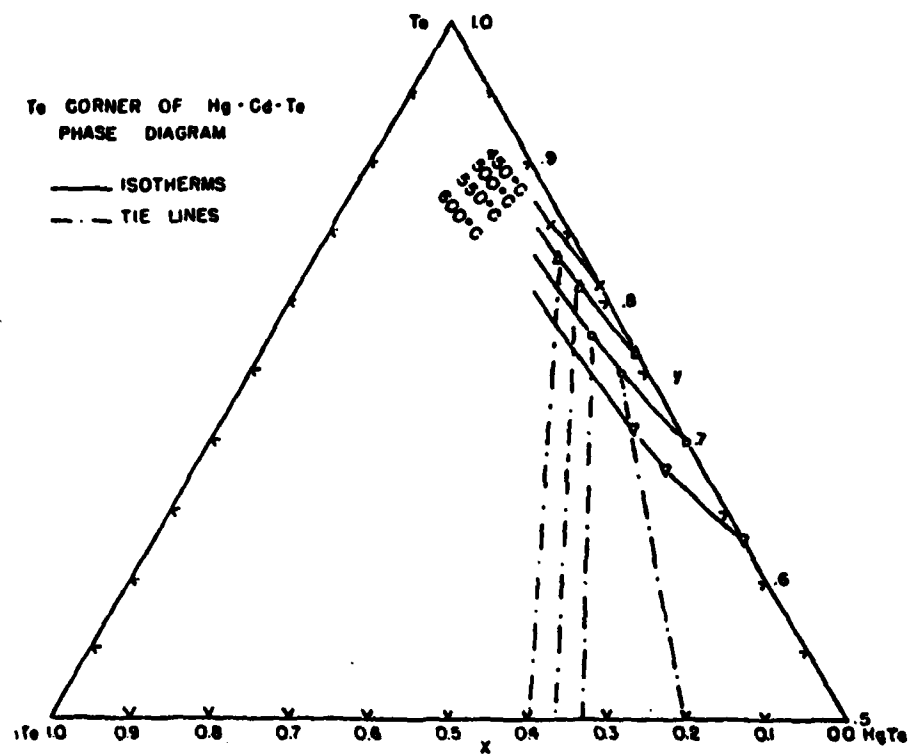


Figure 4. Ternary Phase Diagram for Te-CdTe-HgTe. Shows four experimentally determined liquidus isotherms and four tie lines.

Table 1. Composition of LPE Layers

Growth Run	EDAX	Lattice Constant	Transmission
23	0.40	0.39	0.38
25	0.39		
28	0.40		

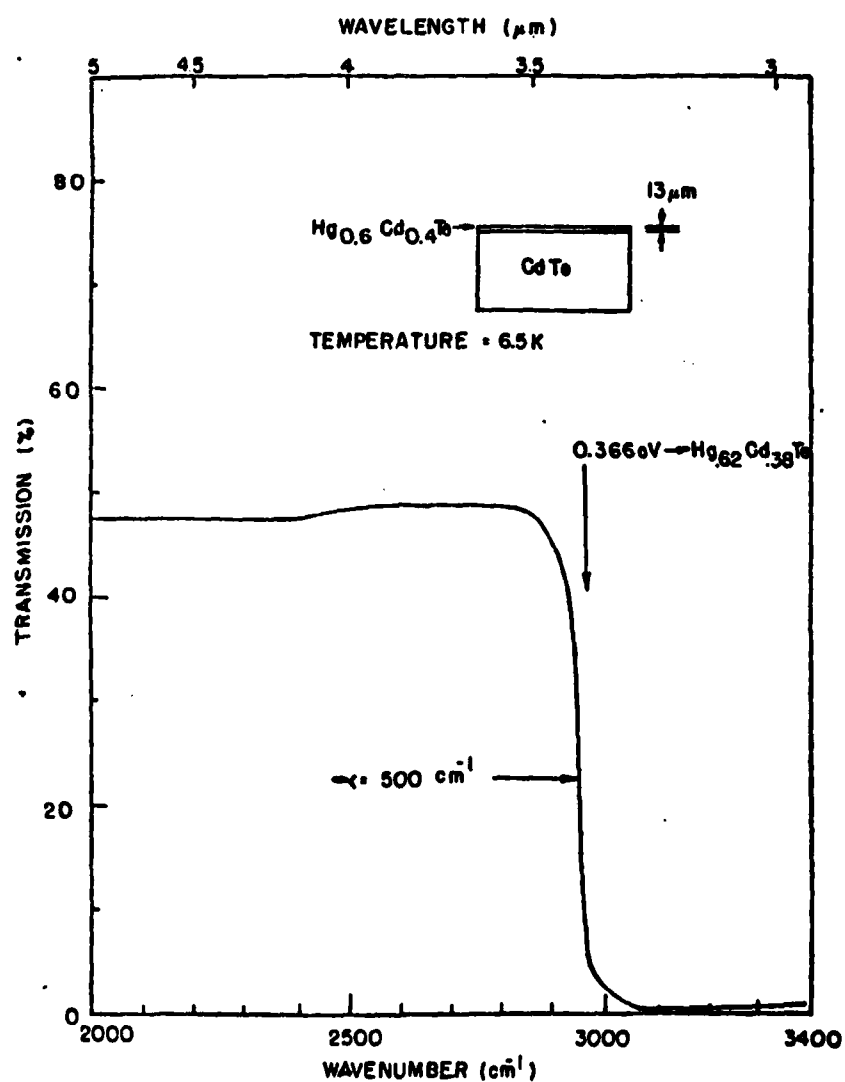


Figure 5. Transmission Curve. This curve as a function of energy for a 13 μm thick LPE film on 1mm of CdTe.

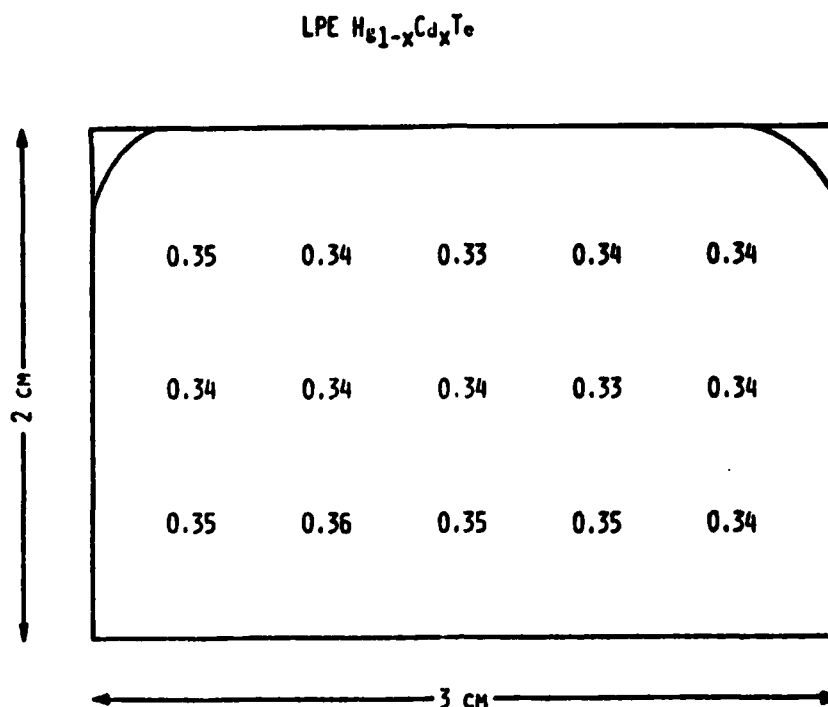


Figure 6. Map of Composition. Composition in mole fraction CdTe as a function of position across a  $2 \times 3 \text{ cm}^2$  LPE grown layer.

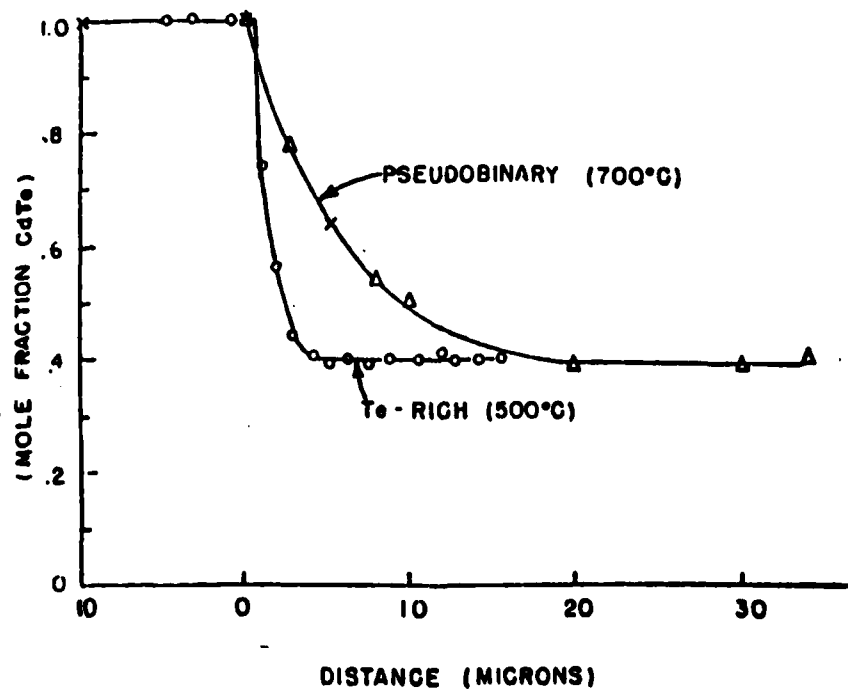


Figure 7. Profile of Composition. Composition as a function of Depth into LPE layers grown at 500°C and 700°C.

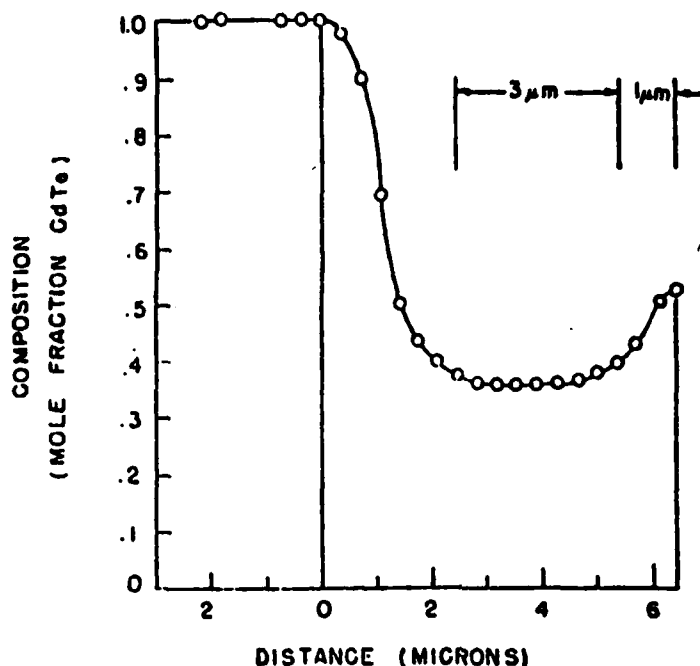


Figure 8. Profile of Composition. Compositional profile of a double LPE layer grown at 500°C.

The surface morphology of most of the layers we have grown is good. Early layers had from  $10^6$  to  $10^7$  pinholes per  $\text{cm}^2$ , but better purging with high purity  $\text{H}_2$  gas at 500 cc/min overnight reduced pinhole density to  $\sim 45/\text{cm}^2$ . The layers are microscopically smooth but are not optically flat having gentle undulations of  $< 1\mu\text{m}$  amplitude and a period of  $\sim 20\mu\text{m}$ . We rarely see terracing or steps across a surface. Cleaved  $40\mu\text{m}$  thick LPE layers of  $\text{Hg}_{0.8}\text{Cd}_{0.2}\text{Te}$  appear to have perfectly smooth growth interfaces at 40x magnification. We have grown layers within  $0.1^\circ$  of the (111)A and (111)B orientations and within  $1.5^\circ$  of the (111)A, (111)B and the (100) orientations and have found no measurable differences. Most of our layers have been grown on the (111)A and B orientations since it is easier to cut large single crystals parallel to the (111) twin planes. We have grown layers across a twin boundary and find a vee-trough in the grown layer  $\sim 3\mu\text{m}$  deep at the center and  $40\mu\text{m}$  wide. We have no data on lifetime in such a region.

Electrical properties have been measured on several LPE layers grown from Te-rich solution, both before and after annealing in Hg vapor. The  $\text{Hg}_{0.8}\text{Cd}_{0.2}\text{Te}$  films generally

are p-type as grown with 77K mobility of  $\sim 10^4 \text{cm}^2/\text{Vs}$ . After annealing, the mobility increases to 2 to  $4 \times 10^6 \text{cm}^2/\text{Vs}$  indicating a reduced acceptor concentration. Considering the combination of mixed conduction and surface inversion complicating the interpretation of the Hall data<sup>16</sup>, net acceptor concentrations after annealing are estimated to be  $\sim 10^{15} \text{cm}^{-3}$ . Layers of  $\text{Hg}_{0.6}\text{Cd}_{0.4}\text{Te}$  have an acceptor concentration of  $\sim 10^{17} \text{cm}^{-3}$  as grown and convert to n-type upon annealing in Hg vapor for an hour at  $300^\circ\text{C}$ . The donor concentration is  $\sim 4 \times 10^{15} \text{cm}^{-3}$  but the 77K mobility of  $\sim 5000 \text{cm}^2/\text{Vs}$  is lower than expected by a factor of four.

We have not yet measured lifetime on the LPE films grown from Te-rich solutions, so we have taken data on earlier films grown from HgTe-rich solutions. Figure 9 is a plot of minority carrier lifetime as measured by the reverse recovery technique as a function of temperature. The upper curve is for three diodes made in an LPE film<sup>17</sup> while the lower curves are typical of diodes made in bulk  $\text{Hg}_{1-x}\text{Cd}_x\text{Te}$ .<sup>18</sup> Note that the LPE films show longer lifetime. It is premature to say that LPE material is superior to bulk-grown material but the prospects are exciting.

#### 4. CONCLUSION

In this paper we have outlined techniques suitable for determining liquidus temperature, tie lines, composition and lifetime. We have demonstrated the growth of  $1 \times 1$ ,  $1 \times 4$ , and  $2 \times 3 \text{ cm}^2$  LPE films of  $\text{Hg}_{1-x}\text{Cd}_x\text{Te}$  with  $0.2 < x < 0.4$  uniform in composition across the surface and into the layers. We have shown that these layers are of reasonably low impurity content and that minority carrier lifetime can be longer in LPE-grown material than in bulk grown material of the same composition. We conclude that LPE-grown  $\text{Hg}_{1-x}\text{Cd}_x\text{Te}$  is a viable alternative to bulk-grown material for some applications. For arrays requiring large areas, lower defect concentrations, or multiple layers of different compositions, LPE growth may provide the only viable approach. Further development of LPE growth is still required.



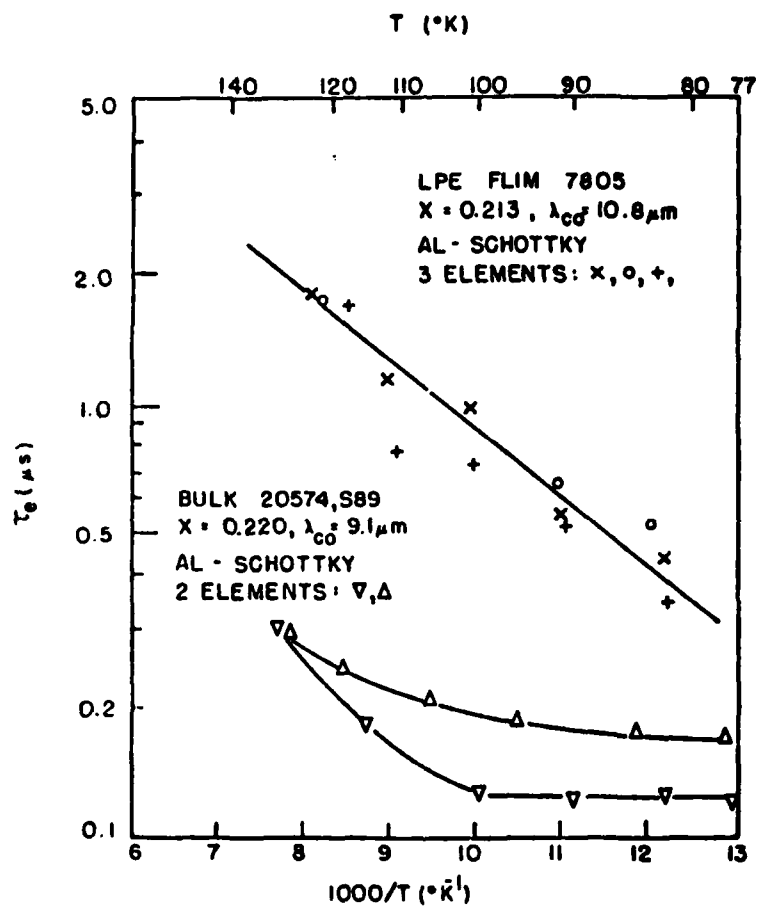


Figure 9. Minority Carrier Lifetime. Minority carrier lifetime measured in Schottky barrier diodes in bulk and in LPE grown  $Hg_{1-x}Cd_xTe$ .

## References

1. T. C. Harman, *Jour. Elec. Mat.* 8, p. 191 (1979).
2. M. Lanir, C. C. Wang, and A. H. B. vanderWyck, *Appl. Phys. Lett.*, 34, p. 50 (1979).
3. J. L. Schmit and J. E. Bowers, "LPE Growth of  $\text{Hg}_{0.6}\text{Cd}_{0.4}$  from Te-rich Solutions," submitted to *Appl. Phys. Lett.*
4. J. E. Bowers, J. Schmit, C. J. Speerschnneider and R. B. Maciolek, "Comparison of  $\text{Hg}_{1-x}\text{Cd}_x\text{Te}$  LPE Layer Growth from Te-, Hg-, and HgTe-rich Solutions," submitted to *IEEE Electron Devices Special Issue on ir Devices*.
5. C. J. Speerschnneider and R. B. Maciolek, Final Report on Contract DAHC60-70-C-008 covering the period May 1971 through May 1973.
6. J. A. Mroczkowski, Final Report on Contract DAAG46-78-C-0020, dated March, 1979.
7. J. P. Schwartz, Ph.D. Thesis, Marquette University, p. 99 (1977).
8. J. C. Woolley and B. Ray, *Jour. Phys. Chem. Solids* 13, p. 151 (1960).
9. M. W. Scott, *Jour. Appl. Phys.* 40, p. 4077 (1969).
10. J. L. Schmit and E. L. Stelzer, *Jour. Appl. Phys.* 40, p. 4865 (1969).
11. R. H. Kingston, *Proc. IRE* 42, 829 (1954).
12. J. L. Schmit, S. P. Tobin and T. J. Tredewell, AFML-TR-79-4036.
13. H. J. Kuno, *IEEE Trans. on El. Dev.*, ED 11, p. 8 (1964).
14. T. C. Harman, *Physics and Chemistry of II-VI Compounds*, Edited by M. Aven and J. S. Premmer, p. 784 (Wiley, New York, 1967).
15. J. Blair and R. Newham, "Metallurgy of Elemental & Compound Semiconductors," Vol. 12, p. 393., (Wiley, New York, 1961).
16. Walter Scott and R. J. Hager, *Jour. Appl. Phys.* 42, p. 803 (1971).
17. Dennis L. Polla, Bachelor's Thesis, MIT, June 1979.
18. A.K. Sood and T.J. Tredwell, Final Report on DAAK70-76-C-0237, March 1978.

**Appendix C**

**Comparison of  $\text{Hg}_{0.6}\text{CD}_{0.4}\text{Te}$  LPE Layer**

**Growth from Te-, Hg- and HgTe-Rich Solutions**

**J. E. Bowers, J. L. Schmit, C. J. Speerschneider and**  
**R. B. Maciolek**

**Honeywell Corporate Technology Center**  
**Bloomington, Minnesota**

**This work was partially supported by the Air Force Materials Laboratory under contract F33615-77-C-5142.**

**Published in the IEEE Transactions on Electron Devices in the January, 1980 special issue on infrared.**

# Comparison of $\text{Hg}_{0.6}\text{Cd}_{0.4}\text{Te}$ LPE Layer Growth from Te-, Hg-, and HgTe-Rich Solutions

JOHN E. BOWERS, STUDENT MEMBER, IEEE, JOSEPH L. SCHMIT, CHARLES J. SPEERSCHNEIDER,  
AND RALPH B. MACIOLEK

**Abstract**— $\text{Hg}_{1-x}\text{Cd}_x\text{Te}$  has been grown on CdTe substrates by liquid-phase epitaxy (LPE) from: 1) Te-rich solution at atmospheric pressure in a slider system, 2) Hg-rich solution in a sealed tube dipping system, and 3) HgTe-rich solution in sealed tube tipping and sliding systems. For epitaxial layers grown from Te-rich solution at 500°C, the width of the graded composition region is 3  $\mu\text{m}$  and the compositional variation across the layer and with depth into the layers is less than  $\pm 0.01$  mole fraction CdTe. The graded composition region for layers grown from Hg-rich solution at 460°C is less than 3  $\mu\text{m}$ ; however, there is no uniform composition region because of CdTe depletion from the melt. The graded bandgap region for pseudobinary growth at 700°C is much wider (20  $\mu\text{m}$ ) than the other two cases; however, a region of uniform composition can be obtained by growing sufficiently thick layers ( $> 30 \mu\text{m}$ ). Pseudobinary growth has the theoretical advantage that either p-type or n-type layers may be grown, whereas, only p-type layers may be grown from Te-rich solution at atmospheric pressure.

## I. INTRODUCTION

THE SEMICONDUCTOR  $\text{Hg}_{1-x}\text{Cd}_x\text{Te}$  is important for use in photovoltaic and photoconductive infrared photo-detectors [1], [2]. Most of the material for infrared devices is currently prepared by controlled solidification of the molten alloy at a relatively high temperature (800°C), followed by a homogenization anneal (650°C), and when necessary, a low-temperature anneal (300°C) to adjust crystal stoichiometry [3]–[6].

Liquid-phase epitaxy (LPE) overcomes the compositional nonuniformity inherent in the nonequilibrium solidification of this pseudobinary alloy and the long anneal times required to restore homogeneity. LPE techniques also have the advantage that multiple layers of  $\text{Hg}_{1-x}\text{Cd}_x\text{Te}$  can be grown with different compositions and doping levels. Multilayer structures are advantageous for the fabrication of monolithic  $\text{Hg}_{1-x}\text{Cd}_x\text{Te}$  detectors and CCD's and also for hybrid devices using  $\text{Hg}_{1-x}\text{Cd}_x\text{Te}$  detectors mated to silicon CCD's. Because of the low Hg vapor pressure inherent in growth from Te-rich solution, large-diameter growth tubes may be used. Consequently, there is the possibility of growing large-area epitaxial layers for future cost-effective focal plane arrays. These large arrays cannot be obtained from bulk growth since the quartz-tube cross-sectional area must be limited to several square centi-

meters to withstand the high Hg pressures present at temperatures around 800°C.

LPE growth of  $\text{Hg}_{1-x}\text{Cd}_x\text{Te}$  from Te-rich solution has recently been reported [7]–[9]. In this paper, we report results of growth from Te-, Hg-, and HgTe-rich solutions and state the relative advantages and disadvantages of each approach. The compositional uniformity of the layers and limits to the compositional uniformity in each case are discussed. Electrical characteristics of the layers are presented.

## II. EXPERIMENTAL PROCEDURE

The three methods used in this investigation for bringing the melt and substrate in contact are: 1) sliding the melt on and off the substrate [10], 2) tipping the melt on and off the substrate [11], and 3) dipping the substrate into the melt [12].

A sliding apparatus in a quartz tube at atmospheric pressure was used for the Te-rich growth. The epitaxial layers were grown isothermally in flowing  $\text{H}_2$  at 500 and 460°C. The Hg pressure over these solutions was  $< 0.1$  atm [13] and growth times were kept  $< 30$  min to minimize Hg loss. The substrates were chemimechanically polished (111) *A* and *B* faces of CdTe of 1-cm<sup>2</sup> area.

The Hg-rich growths were done in sealed, evacuated quartz tubes using a dipping system. The layers were grown at 460°C on 8-mm-diameter CdTe substrates.

Both tipping and sliding systems in sealed evacuated quartz tubes were used in growths from HgTe-rich solution. Growths at 700°C on both CdTe and Si substrates were made. Excess Hg was added to the quartz tubes to provide the necessary Hg pressure.

The compositions and compositional profiles were determined using electron-beam microprobe by comparing the X-ray fluorescence from the layers to reference samples whose composition was determined by density measurements. The experimental error was  $\pm 0.01$  mole fraction CdTe. Measurements of the cutoff wavelength and X-ray determination of the lattice constant confirmed the LPE layer composition. The carrier concentrations and mobility values were determined by van der Pauw–Hall coefficient measurements.

Te-rich phase diagram data were determined from differential thermal analysis (DTA) measurements and LPE growth results. Only the LPE growth results are reported because supercooling makes the interpretation of the DTA results uncertain to  $> 25^\circ\text{C}$ . The Hg-rich points were determined by two different techniques. In one method, the solution was cooled in steps and checked each time for nucleation of a solid phase. Once this appeared, the alloy was quenched and the

Manuscript received May 8, 1979; revised August 6, 1979. This work was partially supported by the Air Force Materials Laboratory under Contract F33615-77-C-5142.

J. E. Bowers, J. L. Schmit, and C. J. Speerschnieder are with Honeywell Corporate Technology Center, Bloomington, MN.

R. B. Maciolek was with Honeywell Corporate Technology Center, Bloomington, MN. He is now with Minnesota Mining and Manufacturing, St. Paul, MN.

composition of the solid was determined by electron-beam microprobe. This method gives good values for the compositions of the liquid and solid phases, but the unknown degree of supercooling limits the accuracy of the measured liquidus temperature to  $\pm 25^\circ\text{C}$ . The second method used for Hg-rich phase diagram measurements kept an  $\text{Hg}_{1-x}\text{Cd}_x\text{Te}$  seed in contact with a solution for a long time at constant temperature, and then the solution and seed were quenched. The composition of the surface of the seed and the loss of HgTe and CdTe from the seed were measured. This technique complements the first in that it gives accurate values for the liquidus temperature and solidus composition, but the solution composition is not as well known.

### III. RESULTS AND DISCUSSION

#### A. Ternary Phase Diagram

The ternary phase diagram for  $\text{Hg}_{1-x}\text{Cd}_x\text{Te}$  is shown schematically in Fig. 1. A given composition (such as  $\text{Hg}_{0.6}\text{Cd}_{0.4}\text{Te}$ ) can be grown from Te-rich solution (line *a*), from Hg-rich solution (*b*), or from HgTe-rich solution along the pseudobinary line (*c*). A big difference between these approaches is the Hg pressure present in each case. From the solidus data of Schwartz and Brebrick [13] given in Fig. 2, it can be seen that the Hg vapor pressure at  $500^\circ\text{C}$  over Te saturated  $\text{Hg}_{0.6}\text{Cd}_{0.4}\text{Te}$  is 0.1 atm. Adding Te to this solid does not change the equilibrium Hg vapor pressure [13]. Consequently, standard LPE techniques [14] developed for the growth of III-V semiconductors can be used with slight modification to provide or contain the necessary Hg. The Hg vapor pressure over an Hg-rich solution (7 atm at  $500^\circ\text{C}$ ) is much higher than over a Te-rich solution. This requires the use of either sealed quartz tubes or high-pressure fittings. The equilibrium Hg pressure can, of course, be reduced by adding Hg to the solution and lowering the liquidus temperature. In principle,  $\text{Hg}_{1-x}\text{Cd}_x\text{Te}$  could be grown at 0.1 atm Hg pressure from Hg-rich solution at  $250^\circ\text{C}$  although the low solubility of Cd and Te would make growth impractically slow. For growth from HgTe-rich solution, the Hg vapor pressure will be that of the liquidus composition required to give the desired solid composition. The melting point of HgTe is  $671^\circ\text{C}$  [15], so the minimum Hg pressure possible is  $\sim 10$  atm.

Tie lines for the Hg-rich and Te-rich region of the ternary phase diagram are shown in Fig. 3, and these data together with the associated liquidus temperatures are listed in Table I. From this diagram, it is clear that growth from Cd-rich melts produces a solid that is essentially all CdTe. We do not have enough data on any one composition to plot liquidus and solidus curves versus temperature.

A problem with low-temperature Hg-rich growth is that there is much less Cd in a Hg-rich solution than in an equivalent Te-rich solution. Consider, for example, using a 1-g Te-rich solution (data point *F* in Table I) to grow a layer of composition  $x = 0.35$ , thickness: 10  $\mu\text{m}$ , and  $1\text{-cm}^2$  area. This consumes 7 percent of the Cd in the melt. Based on our limited phase diagram data, this should produce a compositional variation in the epitaxial layer of 0.01 mole fraction due to Cd depletion. However, to grow the same layer from a 1-g Hg-rich melt at  $450^\circ\text{C}$  (data point *C* in Table I), 75 percent of the Cd would be consumed. Thus from phase diagram considerations, we ex-

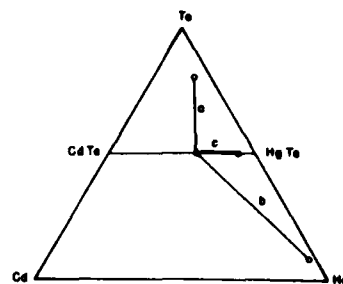


Fig. 1. Schematic Hg-Cd-Te ternary phase diagram. Three solutions are shown which are in equilibrium with  $\text{Hg}_{0.6}\text{Cd}_{0.4}\text{Te}$ .

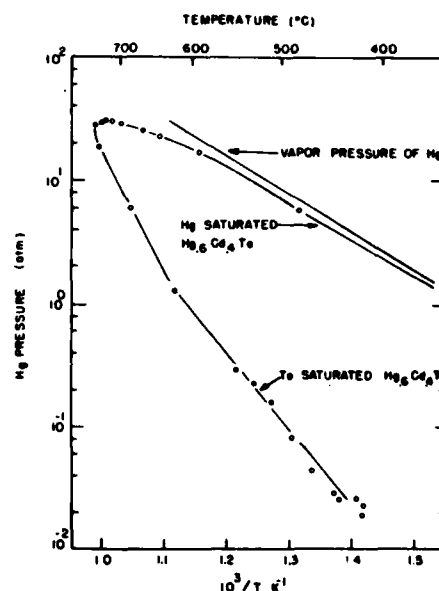


Fig. 2. Partial pressure of Hg over Hg-saturated and Te-saturated  $\text{Hg}_{0.6}\text{Cd}_{0.4}\text{Te}$  (after Schwartz [13]).

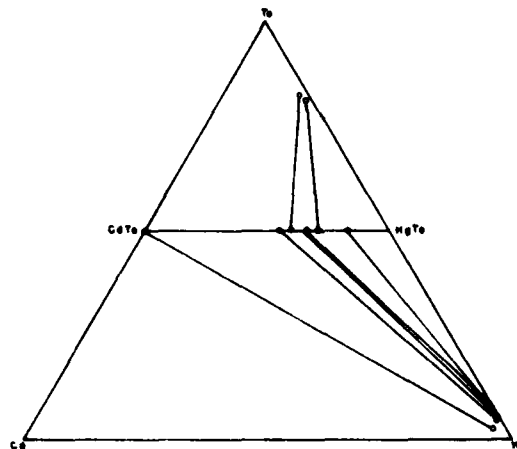


Fig. 3. Hg-Cd-Te ternary phase diagram.

TABLE I  
PHASE DIAGRAM DATA FOR THE TERNARY Hg-Cd-Te

Data Point	Temperature (°C)	Liquidus			$x_{\text{solid}}$ Hg-Cd-Te (mole fraction of each)	$k$ ( $C_d/C_{d0}$ )	$p_{\text{Hg}}^{(13)}$ (atm)
		Hg	Cd	Te			
		(mole fraction of each)					
A	450 ± 25	0.924	0.004	0.072	0.17 ± 0.03	21	4
B	460 ± 2	0.890	0.007	0.103	0.14 ± 0.02	24	19
C	450 ± 25	0.950	0.002	0.048	0.35 ± 0.05	87	4
D	506 ± 2	0.947	0.009	0.044	0.45 ± 0.05	25	7
E	475 ± 25	0.950	0.025	0.025	1.00 ± 0.05	20	5
F	509 ± 2	0.180	0.016	0.804	0.29 ± 0.02	11	0.1
G	507 ± 2	0.157	0.018	0.825	0.40 ± 0.01	11	0.1

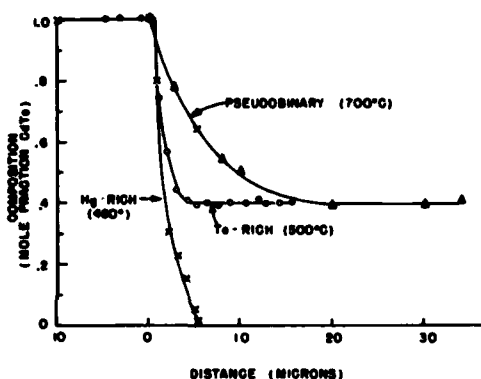


Fig. 4. Compositional profiles for layers grown from Te-, Hg-, and HgTe-rich solutions.

pect a large compositional variation due to Cd depletion in Hg-rich solutions, but a small variation in epitaxial layers grown from Te-rich solutions. The Cd segregation coefficient for HgTe-rich solutions is even less than that for Te-rich solutions, so we expect no detectable compositional variation due to Cd depletion for pseudobinary grown layers less than 50  $\mu\text{m}$  thick.

#### B. Compositional Profiles

The compositional profiles of three typical layers grown from Te-, Hg-, and HgTe-rich solutions are shown in Fig. 4. We wish to determine if the width of the graded composition regions is limited by interdiffusion. It is difficult to calculate an interdiffusion profile since the diffusion constant depends strongly on composition. However, following the work of Bailly *et al.* [16]–[18], it is relatively easy to calculate diffusion coefficients from the compositional profile using Boltzmann's technique [19]. If the calculated diffusion coefficients are higher than the diffusion coefficients obtained by Bailly, then the profile is not due to interdiffusion. The values for diffusion coefficients obtained by Bailly [16],<sup>1</sup> are

<sup>1</sup> Our epitaxial layers were grown on In-doped semi-insulating CdTe so Bailly's data for diffusion between HgTe- and In-doped semi-insulating CdTe were used for comparison.

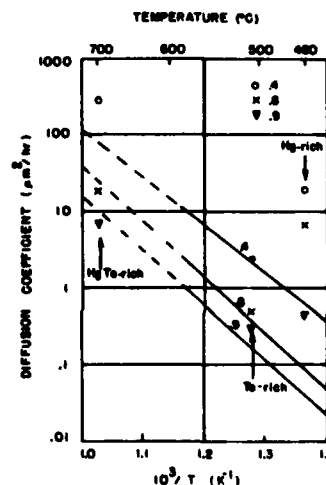


Fig. 5. HgTe-CdTe interdiffusion coefficient for several different CdTe mole fractions ( $x = 0.4, 0.8$ , and  $0.9$ ). Bailly's data [16] are represented by solid lines.

shown in Fig. 5 along with our calculated diffusion coefficient values. The values of the diffusion coefficient for three different CdTe concentrations ( $x = 0.4, 0.8, 0.9$ ) are shown. The dotted lines are extrapolations of Bailly's data. This discussion ignores the weak dependence of diffusion coefficient on Hg pressure; however, the same conclusions are reached when this effect is taken into account.

1) *Hg-Rich Growth*: The narrowest graded composition region was obtained for Hg-rich growth at 460°C. However, there is no constant composition region for layers grown from Hg-rich solutions at low temperatures as expected from the phase diagram considerations given earlier. Our values of diffusion coefficient in layers grown from Hg-rich solution are two orders of magnitude higher than Bailly's values. We conclude that the slope of the composition profile for Hg-rich growth is not limited by interdiffusion. Note that the surface composition is HgTe indicating a complete loss of Cd at least at the growth interface.

2) *Te-Rich Growth*: The compositional profile of a layer grown from Te-rich solution has a 13- $\mu\text{m}$ -wide uniform com-

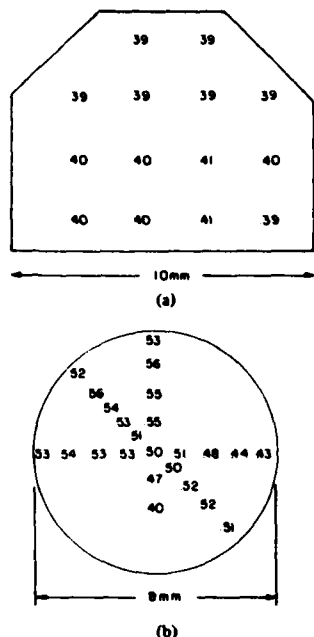


Fig. 6. Variation of CdTe mole fraction across the epitaxial layer surface. (a) Layer grown from Te-rich solution. (b) Layer grown from HgTe-rich solution.

position region as expected from phase diagram considerations. The diffusion coefficients calculated from the graded composition region (Fig. 5) are close to those obtained by Bailly, so we conclude that the  $3\text{-}\mu\text{m}$ -wide graded composition region is due to interdiffusion. A Te-rich growth at  $460^\circ\text{C}$  produced an epitaxial layer with only a  $1\text{-}\mu\text{m}$ -wide interdiffusion region, and again the calculated diffusion coefficients were comparable to Bailly's values.

The compositional uniformity across the surface of a layer is shown in Fig. 6(a). The variation of  $\pm 0.01$  mole fraction CdTe is within the electron-beam microprobe experimental error.

We have found no measurable difference between layers grown on (111)A, (111)B, and a random orientation.

3) *Pseudobinary Growth*: Uniform composition layers may be grown from HgTe-rich solution, provided the layers are more than  $30\text{ }\mu\text{m}$  thick (Fig. 4). The calculated values for diffusion coefficients agree with Bailly's values, particularly for  $x = 0.8$  and  $0.9$ . Consequently, the shape of the high  $x$  region is probably determined by interdiffusion.

The compositional profile of a  $\text{Hg}_{1-x}\text{Cd}_x\text{Te}$  layer grown from HgTe-rich solution on a silicon substrate is shown in Fig. 7. The excellent uniformity of this layer proves that Cd depletion from the melt does not cause the nonuniformity present in growth from HgTe-rich solution. Although the uniformity of this layer is excellent, growth on silicon substrates was not pursued because of the large lattice mismatch (16 percent) and difficulty obtaining epitaxial growth.

Hg vapor transport to the CdTe substrate surface during the 1-h time allowed for the solute to dissolve at  $770^\circ\text{C}$  produces

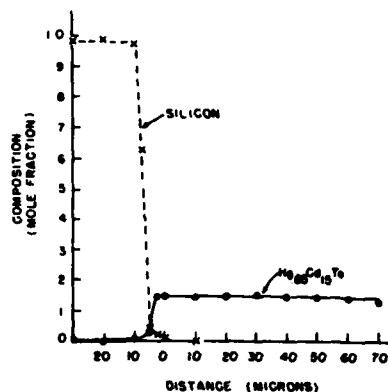


Fig. 7. Compositional profile of a  $\text{Hg}_{0.85}\text{Cd}_{0.15}\text{Te}$  layer grown from a HgTe-rich solution on an Si substrate.

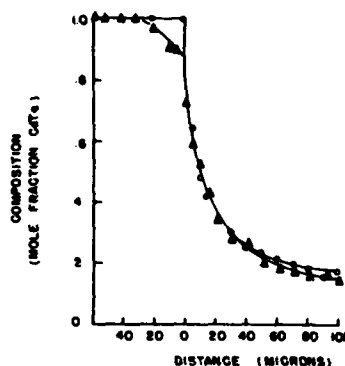


Fig. 8. Compositional profiles of layers grown from HgTe-rich solution with meltback before growth (circles) and without meltback (triangles).

a graded composition region [20] before growth is initiated. It was found that a substrate taken through the entire growth sequence, except that a melt was not tipped onto the substrate, had a surface composition of  $x = 0.8$ . The compositional profiles of a layer grown on a melted-back substrate and a layer grown without meltback are compared in Fig. 8. It can be seen that significant rounding occurs at the substrate-layer interface. The HgTe-rich grown layer whose profile was given in Fig. 4 was grown on a melted-back substrate.

The same effect occurs for Hg-rich and Te-rich growth, but the diffusion coefficient is much smaller at  $450^\circ\text{C}$  so the effect was not detectable.

The variation of composition across the surface of a layer is shown in Fig. 6(b). The uniformity is not as good as for the layer grown from Te-rich solution.

### C. Electrical Properties

Epitaxial layers grown at  $500^\circ\text{C}$  from Te solution were found to be p-type with a carrier concentration of  $1 \times 10^{17}/\text{cm}^3$ . An anneal at  $300^\circ\text{C}$  in Hg vapor converted a layer to n-type with a carrier concentration of  $4 \times 10^{18}/\text{cm}^3$ . This is in agreement with the annealing studies of Schmit and Stelzer [21] on

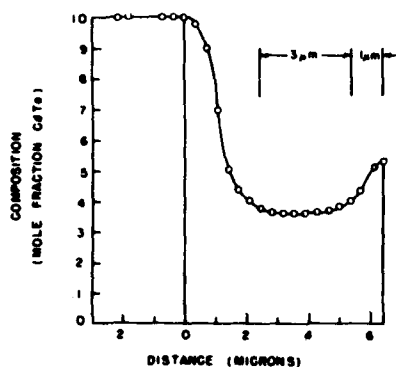


Fig. 9. Compositional profile of double-layer structure.

bulk  $\text{Hg}_{0.6}\text{Cd}_{0.4}\text{Te}$ . They also found that annealing in Hg vapor is necessary to significantly reduce the hole concentration or convert the material to n-type. Consequently, the limitation of an open tube system is that only p-type layers can be grown and a separate anneal in a sealed tube with free Hg must be used to convert the layers. Alternately, n-type dopants could be added to the growth solution to compensate the stoichiometric acceptors.

The limitation to as-grown p-type layers does not exist with HgTe-rich or Hg-rich growth. From Schmit and Stelzer's paper [22], we expect a p-type layer with a carrier concentration of  $7 \times 10^{16} \text{ cm}^{-3}$  for growth at  $700^\circ\text{C}$  in Hg vapor and quenching to room temperature. However, by cooling the layer more slowly and thus *in situ* annealing the layer, we have obtained both p- and n-type layers.

#### D. Multilayer Growth

There is considerable interest in monolithic infrared detectors coupled to CCD's. In one scheme, the surface CCD layer would have a standard composition such as  $\text{Hg}_{0.5}\text{Cd}_{0.5}\text{Te}$  or CdTe, and the 5-10- $\mu\text{m}$ -thick detector layer would have a different composition, depending on the desired cutoff wavelength.

An advantage of LPE growth over bulk growth is that structures with multiple layers of different compositions and/or doping levels may be obtained. In principle, multiple layers can be grown from Hg- or HgTe-rich solution in a sealed tube; however, these systems are considerably less flexible than open tube Te-rich growth. We have used the latter approach to grow a double-layer structure. The compositional profile of this structure is shown in Fig. 9. The interdiffusion regions are  $2 \mu\text{m}$  wide, and the detector layer has a width of  $4 \mu\text{m}$ . Both layers are p-type and have mirror-like surfaces with pinhole densities less than  $50 \text{ cm}^{-2}$ . Pinholes originate at the substrate, are  $<4 \mu\text{m}$  across, and presumably are the result of inadequate surface preparation since they occur on both sides of the layer boundaries.

#### IV. CONCLUSIONS

Growth from Te solution produces layers with excellent compositional uniformity. The  $3\text{-}\mu\text{m}$  width of the graded bandgap region is due to interdiffusion and may be reduced by growing at lower temperatures. The layers are p-type with a carrier concentration of  $1 \times 10^{17} \text{ cm}^{-3}$  and may be annealed to n-type with a carrier concentration of  $4 \times 10^{15} \text{ cm}^{-3}$ . A multilayer structure was grown.

Layers grown from HgTe-rich solution have uniform composition regions, but wider graded composition regions than Te- or Hg-rich solutions. This is due to increased interdiffusion at the higher growth temperatures required with this technique. Pseudobinary growth has the advantage that n- or p-type layers with a variety of carrier concentrations may be grown.

For growth from Hg-rich solution at  $460^\circ\text{C}$ , the width of the graded bandgap region is not limited by interdiffusion. Uniform composition regions were not obtained with this technique.

#### ACKNOWLEDGMENT

The authors wish to thank W. Scott and R. J. Stokes for helpful discussions, and R. George, R. Skogman, S. J. Marquardt, and J. R. Nelson for technical assistance.

#### REFERENCES

- [1] D. Long and J. L. Schmit, in *Semiconductors and Semimetals*, vol. 5, R. K. Willardson and A. C. Beer, Eds. New York: Academic Press, 1970, p. 175.
- [2] R. Dornhaus and G. Nimtz, *Solid State Physics* (Springer Tracts in Modern Physics), vol. 78. Berlin: Springer, 1976, p. 1.
- [3] J. C. Wooley and B. Ray, *J. Phys. Chem. Solids*, vol. 13, p. 151, 1960.
- [4] J. Blair and R. Newnham, *Metallurgy of Elemental and Compound Semiconductors*, vol. 12. New York: Wiley, 1961, p. 393.
- [5] T. C. Harman, *Physics and Chemistry of II-VI Compounds*, M. Aven and J. S. Prener, Eds. New York: Wiley, 1967, p. 784.
- [6] P. W. Kruse, *Appl. Opt.*, vol. 4, p. 687, 1965.
- [7] T. C. Harman, *J. Elec. Mat.*, vol. 8, p. 191, 1979.
- [8] M. Lanir, C. C. Wang, and A. H. B. van der Wyck, *Appl. Phys. Lett.*, vol. 34, no. 1, p. 50, 1979.
- [9] J. L. Schmit and J. E. Bowers, *Appl. Phys. Lett.*, vol. 35, p. 457, 1979.
- [10] M. B. Panish, I. Hayashi, and S. Sumski, *IEEE J. Quantum Electron.*, vol. QE-5, p. 210, 1969.
- [11] H. Nelson, *RCA Rev.*, vol. 24, p. 603, 1963.
- [12] L. R. Dawson and J. M. Whelan, *Bull. Amer. Phys. Soc. (Ser. 2)*, vol. 13, p. 375, 1968.
- [13] J. P. Schwartz, Ph.D. dissertation, Marquette Univ., Milwaukee, WI, p. 99, 1977.
- [14] L. R. Dawson, *Progress in Solid State Chemistry*, vol. 7, H. Reiss and J. O. McCaldin, Eds. New York: Pergamon, 1972, p. 117.
- [15] J. Steininger, *J. Elec. Mat.*, vol. 5, p. 299, 1976.
- [16] I. Bailly, *C.R. Acad. Sci. Paris*, vol. 262, p. 635, Feb. 28, 1966.
- [17] I. Bailly, G. Cohen-Solal, and Y. Marfaing, *Compt. Rend.*, vol. 257, p. 102, 1963.
- [18] L. Svob, Y. Marfaing, R. Triboulet, I. Bailly, and G. Cohen-Solal, *J. Appl. Phys.*, vol. 46, p. 4251, 1975.
- [19] W. Jost, *Diffusion in Solids, Liquids, Gases*. New York: Academic Press, 1952, p. 31.
- [20] O. N. Tufte and E. L. Stelzer, *J. Appl. Phys.*, vol. 40, no. 11, p. 4559, 1969.
- [21] J. L. Schmit and E. L. Stelzer, *J. Elec. Mat.*, vol. 7, p. 65, 1978.



